LATE QUATERNARY SEDIMENTARY RECORD OF HOLOCENE CHANNEL AVULSIONS OF THE BRAHMAPUTRA RIVER IN THE UPPER BENGAL DELTA PLAIN

By

Jennifer L. Pickering

Thesis

Submitted to the Faculty of the

Graduate School of Vanderbilt University

in partial fulfillment of the requirements

for the degree of

MASTER OF SCIENCE

in

Earth & Environmental Science

May 2013

Nashville, Tennessee

Approved:

Professor Steven L. Goodbred, Jr.

Professor Jessica L. Oster

To my Bangladeshi friends, for the lessons

And to Booly, B-fox, & Little Man

ACKNOWLEDGEMENTS

The research that led to the completion of this thesis would not have been possible without financial support from the National Science Foundation (NSF-OISE-0968354) granted to the BanglaPIRE team, which includes my adviser, Dr. Steven Goodbred, Jr., one of the few academics I know who is able to maintain a positive demeanor and a contagious enthusiasm for this discipline; these traits are certainly responsible, in part, for the truly pleasant experience it was for me to complete this thesis.

Saddam Hossain and Zobayer Mahmood played a huge role in the completion of this research, and I thank them for being such phenomenal field partners. I am indebted to Beth Weinman for first introducing me to the wonder that is the Bengal Delta; to Matthew Cooley and Haley Briel for their time spent in the lab and interest in Himalayan river sediments; and to Warner Cribb for being an exceptional mentor through all of these years. Thanks to Teri Pugh and Jewell Beasley-Stanley, wonderful women with wonderful dispositions, and to Aaron Covey, who has saved my sanity in many a technical crisis. I also thank Dr. Jessica Oster, whose comments greatly improved this thesis. Additionally, thanks to each of the EES faculty and graduate students and to Dr. Manodeep Sinha.

TABLE OF CONTENTS

LIST OF TABLES

LIST OF FIGURES

CHAPTER I

INTRODUCTION

The Bengal basin is an actively evolving depositional environment comprised of unconsolidated muds and sands, which have been transported and deposited by fluvial processes. These sediments form the active channel beds, rice-cultivated floodplains, and highland terraces that make up much of the densely populated country of Bangladesh. As a function of the active tectonics of Himalayan convergence, the region's intense monsoon climate and resultant susceptibility to seasonal flooding, the rivers that have formed this delta are sediment laden and highly mobile.

The stratigraphy of depositional systems can be difficult to decipher due to the dynamism of the processes that form, rework, and ultimately preserve the deposits themselves. In the Bengal basin, the current understanding of Holocene delta formation has been based on relatively few, widely spaced (50-200 km) boreholes, and observational data are still deficient (see e.g., Goodbred and Kuehl, 2000; Nicholls and Goodbred, 2004). In an environment where, for example, the Brahmaputra-Jamuna River channel migrates laterally at rates of at least tens of meters per year (EGIS, 1997), it is necessary to drill systematically positioned, densely sampled transects to capture the complex architecture of the underlying stratigraphy.

As part of a large, 5-year, multi-disciplinary collaborative project that seeks to understand fluvio-deltaic processes under the influence of active tectonics, this study focuses on the first of many closely spaced borehole transects being drilled throughout the Bengal basin. The goal of this transect is to define the latest Pleistocene sea-level lowstand (LPSL) surface in the upper Bengal delta, which represents the distribution of exposed uplands and local incision of the Brahmaputra River and local drainages at a time when sea-level was 120 m lower than today. Secondly, this transect defines the Holocene sediments that have buried the latest Pleistocene boundary and infilled the LPSL valley through the aggradation, avulsion, and lateral migration of the Brahmaputra River.

Motivation and Research Goals

Given the prevalence of geohazards such as earthquakes and riverbank erosion, combined with high population density and the still-developing economy of Bangladesh, it is

especially important to understand the geologic history and behavior of this region. Specifically, it is necessary to define the stratigraphy of the Bengal basin and the processes that have created it in order to understand the tectonic and fluvial processes that regularly affect this small country of over 150 million people. With this goal in mind, we seek to understand the history of the Brahmaputra River that is preserved in the stratigraphic record. Thus, there are three specific objectives guiding this research:

1. Define the LPSL incisional surface in the upper Bengal basin and identify discrete valleys carved by the latest Pleistocene Bengal rivers as sea-level lowered.
2. Determine the width and depth of the LPSL valleys in order to infer the processes, i.e. discrete avulsions or lateral migration, that have built the Holocene stratigraphic fill of these LPSL valleys.
3. Identify the source, lithology, and distribution of sediments preserved in the stratigraphy of the LPSL valleys to reconstruct the history of delta construction since the lowstand.

We have sought to address these goals by drilling a carefully chosen transect of boreholes, Transect A, which consists of 41 boreholes spaced 3 km apart less than 50 km downstream from a recent avulsion node of the Brahmaputra River in northern Bangladesh (Fig. 1). By positioning the transect downstream of an historical avulsion node, the core sites capture the stratigraphy of the two principal Holocene valleys of the Brahmaputra River, which allows us to begin to understand how the Brahmaputra has moved laterally between channel courses since the Last Glacial Maximum (LGM) approximately 20,000 years ago.

Background

The Bengal Basin

The Bengal basin (approximated by the area boxed in blue in Fig. 2A) is situated approximately 200 km south of the Himalaya mountain range and is bordered to the north by the Shillong Anticline, to the west by the Indian Shield, and to the east by the Burma Arc (Fig. 2A). This basin is part of the world's largest depositional system and accommodates almost half of the sediments shed from Himalayan collision (Métivier et al., 1999); eventually, much of this

sediment is transported through the Bengal basin and discharged to the Bay of Bengal and deep-sea Bengal fan.

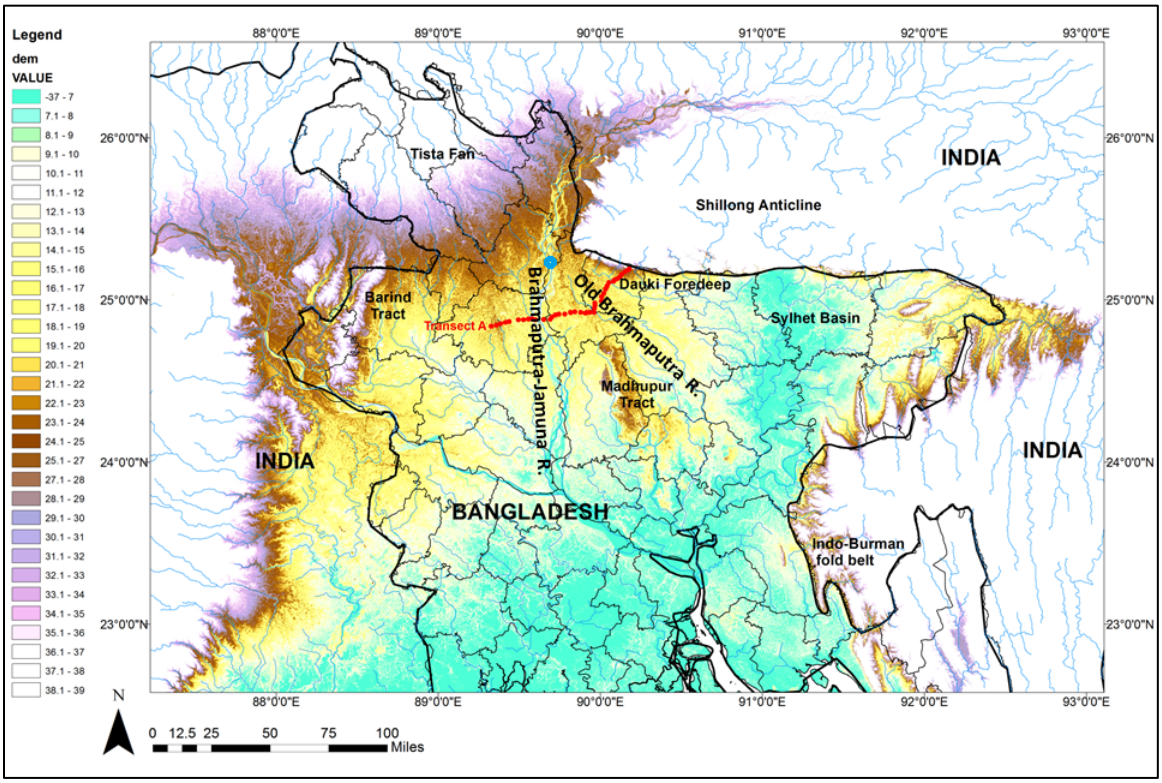

Figure 1: Digital Elevation Model (DEM) of Bangladesh. Relevant geomorphic features are labeled. The blue dot is the most recent avulsion node of the Brahmaputra River.

The Bengal basin, though somewhat flat, is geomorphically and structurally complex. The hinge zone, or the area of maximum curvature associated with transition from the Indian continental shelf to the Bengal foredeep trough, bisects the basin and trends SW-NE through the study area (Fig. 2B). The northwest half of the basin consists of ~8 km of stable shelf deposits (Alam, 1989), and the southeast half is an actively subsiding foredeep with >16 km of unconsolidated deltaic sediment (Curray, 1991).

Basin Structure and Tectonics

The Bengal basin is extensively faulted as evidenced by countless historically and geologically significant earthquakes including the great Assam earthquake of 1897, one of the

ten largest known earthquakes in history. Sukhija et al. (1999) constrained a recurrence interval of 400-600 years between major earthquakes in an area on the north side of the Shillong Anticline (marked as “Shield Area (Shillong Plateau)” on Fig. 2A). Large earthquakes are known to have changed the courses of rivers in this area in the past, e.g. the 1897 Assam earthquake caused the Krishnai River, a tributary of the Brahmaputra, to flood and avulse westward onto land that was higher in elevation than the pre-earthquake path (Oldham, 1899). Eventually the new Krishnai became stable by widening an old drainage channel.

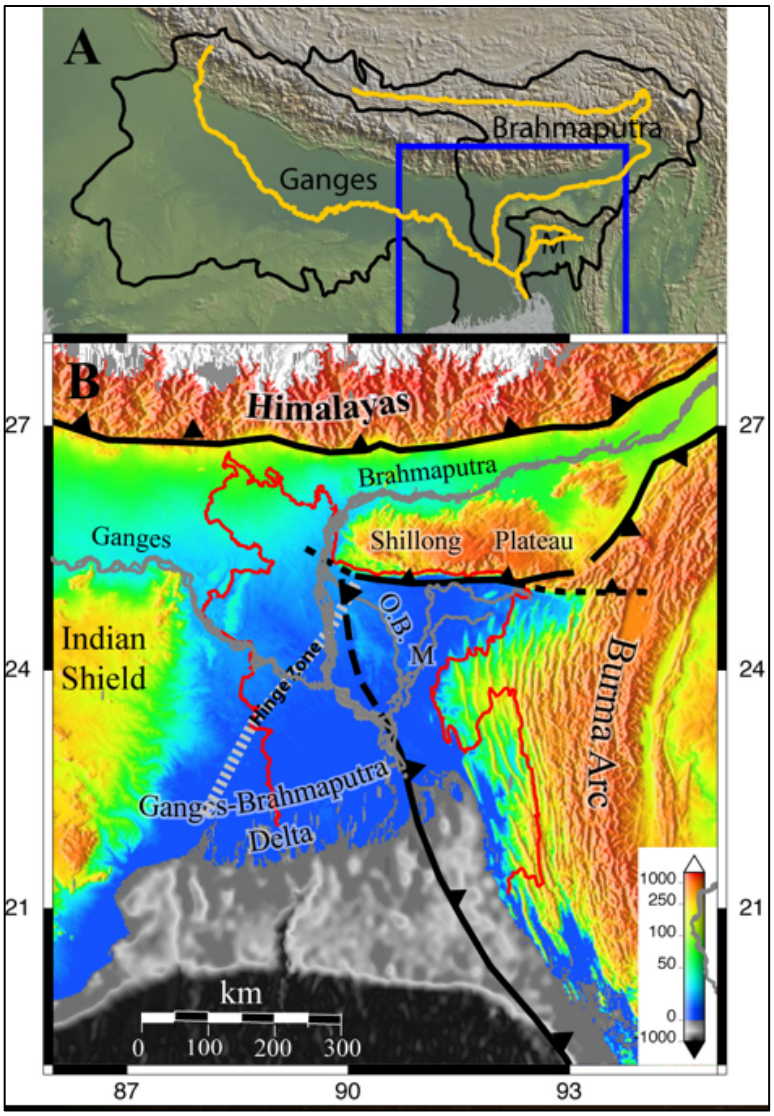

Figure 2: (A) The Ganges, Brahmaputra, and Meghna rivers (shown in yellow) and their catchments, converge in the Bengal basin. The blue box approximates the area of the Bengal basin. (B) DEM of the Bengal basin shown in tectonic context with both the Himalayas and Burma Arc overthrusting the Indian Shield. Bangladesh is outlined in red; O.B. is the Old Brahmaputra River; M is the Meghna River; and the hinge zone represents the transition from continental to oceanic crust on the Indian plate. Modified slightly from a figure provided by Michael Steckler, Lamont-Doherty Earth Observatory, Columbia University.

Basin Hydrology

Three major rivers drain the Bengal basin: the Ganges, the Brahmaputra, and the Meghna (Fig. 2A). After draining Himalayan bedrock, the Ganges and Brahmaputra rivers exit the mountains and become alluvial rivers. They converge in central Bangladesh and join with the Meghna River, which drains the hills of east India and northeast Bangladesh, before discharging into the Bay of Bengal. These rivers are primarily fed by rainfall, typically between 125 and 400 cm/yr, most of which occurs during the monsoon season from June and September. Himalayan pre- and early monsoon snowmelts also contribute significantly (e.g., ~34% annually in the Brahmaputra and <20% annually in the Ganges) to river discharge through the basin (Bookhagen and Burbank, 2010).

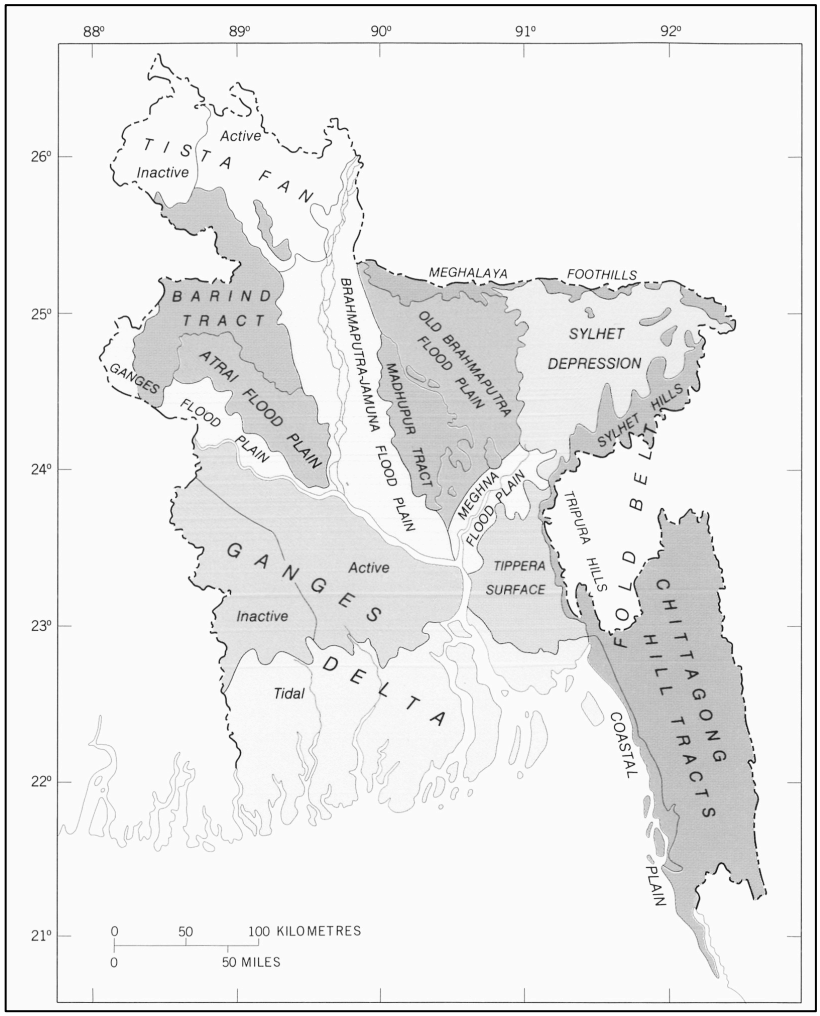

Figure 3: Generalized physiographic map of Bangladesh. From Alam et al., 1990.

The Brahmaputra River

During the late 18th-early 19th century, the Brahmaputra River avulsed, or changed course, at a site ~8 km northeast of the village of Dewanganj in Jamulpur district, near the Tista-Brahmaputra confluence (Fig. 1), in north-central Bangladesh. Within Bangladesh, the current course is known as the Jamuna River (here we refer to the current channel as the Brahmaputra-Jamuna River; "Brahmaputra" is used when referring to the river in general, without regard to either of the recently occupied channels, and the channel occupied prior to ~1800 AD is referred to as the Old Brahmaputra River).

In addition to Himalayan snowmelt and monsoon rainfall, the Brahmaputra River also receives water and sediment input from the Tista River, which drains the topography northwest of Bangladesh and joins the Brahmaputra about 20 km north of the Bahadurabad gauging station near Dewanganj. At the Bahadurabad station, the Brahmaputra-Jamuna has a seasonal water stage difference of ~6 m and bankfull discharge is estimated at 45,000 to 60,000 m^3/s (Table 1; Best et al., 2007). The maximum river depth during flood season is 35 m. Best et al. (2007) note that the Brahmaputra-Jamuna primarily has a braided planform with some vegetated chars that persist over decadal timescales. The modern riverbanks, composed of loosely packed fine sand and silt, are very susceptible to bank erosion (Baki and Gan, 2012), so much so that Thorne et al. (1993) estimated bank erosion rates up to ~200 m/yr between 1953 and 1989. This property also makes the river laterally mobile, and it has widened significantly in the past 3 decades (EGIS, 2000) with braidbelt widths reaching 18 km (Garzanti et al., 2004).

Table 1: Physical characteristics of the Brahmaputra-Jamuna River. Modified from Sarker and Thorne, 2006.

Parameters	Brahmaputra-Jamuna at Bahadurabad
Catchment area (10^3 km^2)	573
Mean annual discharge (m^3 s^{-1})	20,200
Mean annual flood (m^3 s^{-1})	70,000
Slope (cm km^{-1})	8.5 - 6.5
Mean annual sediment load (Mt yr^{-1})	590
Mean annual bed material load (Mt yr^{-1})	200
Median bed material size (D_{50}) (mm)	0.20

The mainstem Brahmaputra-Jamuna acquires ~35% of its sediment load from the Namche Barwa and Great Bend gorge along the Himalayan syntaxis between Tibet and Assam,

India. Budget estimates place another ~5% from the remaining Tibetan landscape; ~14% from the Lohit River and Mishmi Hills of Arunachal Pradesh, India; ~14% from other Himalayan tributaries; and ~7% from the Shillong Anticline and Indo-Burman ranges bordering Bangladesh (Garzanti et al., 2004). Downstream from these tributaries at Bahadurabad, the Brahmaputra has an estimated average sediment load of 590 Mt/yr (Flood Action Plan 24, 1996), comprising approximately 40% silt and 60% sand on the riverbanks and 10% silt and 90% sand on the chars, or island bars within the braidbelt (Thorne et al., 1993).

Modern Physiography of the Bengal Basin

The Barind Tract and Madhupur Tract are pre-Holocene uplands, i.e. weathered floodplain deposits from the last sea-level highstand or before, which flank the modern Brahmaputra-Jamuna floodplain (Fig. 3). The Meghalaya Foothills and Sylhet basin flank the Old Brahmaputra floodplain to the north and east respectively, and the Madhupur Tract flanks the Old Brahmaputra floodplain to the west. The Barind and Madhupur Tracts divide the low-lying Bengal basin into separate sub-basins. This division causes differences in sediment flux to those sub-basins and ultimately contributes to avulsions in the Brahmaputra's course (Goodbred et al., 2003).

The nature of formation of these pre-Holocene uplands has been a topic of debate in recent years that is still largely unresolved. The most comprehensive literature review on the origin and evolution of these features, commonly referred to as Pleistocene terraces, by Rashid et al., (2006) found that some studies interpret these features as floodplain sediments that were deposited during the Pleistocene and have since been tectonically uplifted, while other studies have concluded that the Barind Tract and much of the Madhupur Tract were deposited during the Pleistocene but have since been shaped by river erosion and depositional processes rather than tectonic uplift. Regardless of their evolution, these features are typically 5-7 m higher in elevation than the adjacent alluvial valleys.

The Sylhet Basin in northeast Bangladesh is actively subsiding. The most recent average vertical GPS-measured velocity in Jamulpur District is -6.18 mm/yr (Steckler et al., 2012). This rate is comparable to longer-term Holocene rates of 3-4 mm/yr determined from radiocarbon-dated boreholes (Goodbred and Kuehl, 2000). Although this area has been subsiding throughout the Cenozoic as the Burma Arc to the east overrides the Bengal basin, subsidence rates in Sylhet probably increased substantially in the Pliocene-Pleistocene as the

Shillong Anticline began to overthrust the delta (Johnson and Alam, 1991). As a result of its low elevation and poor drainage, the Sylhet Basin floods extensively during the monsoon season and experiences occasional flash flooding throughout the rest of the year.

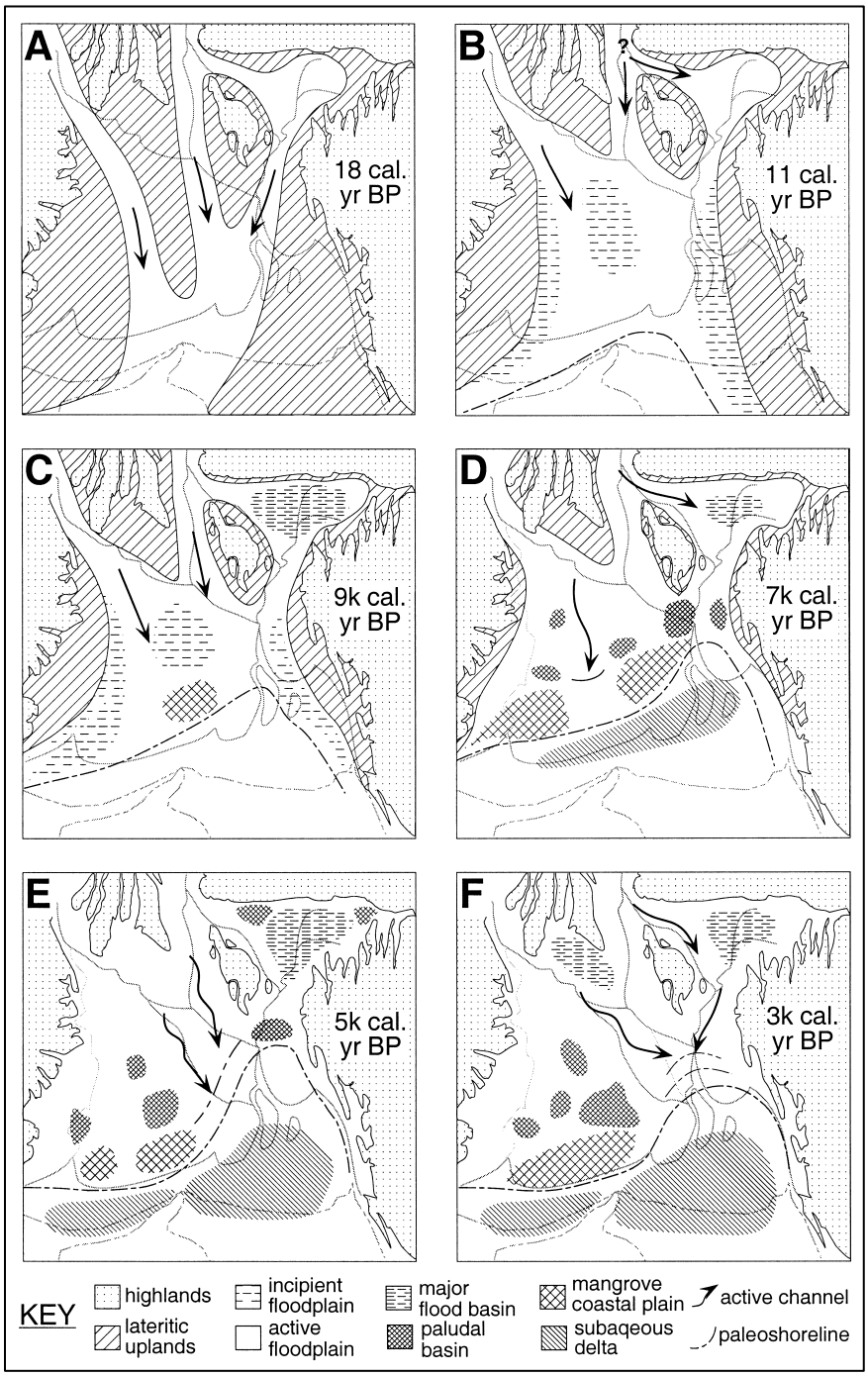

Figure 4: Paleo-physiography of Bengal basin. (A) Latest Pleistocene lowstand geomorphology showing incising river corridors. (B - F) Delta growth and aggradation as sea level rose throughout the Holocene. From Goodbred and Kuehl, 2000.

Late Quaternary Paleo-physiography & Stratigraphy

The work of Goodbred and Kuehl (2000) determined the Late Quaternary paleo-physiography of the Bengal basin. Figure 4 illustrates this physiography at 6 stages throughout the Late Quaternary. During the last lowstand ~18,000 yr BP, the main rivers discharged to the coast through incised valleys that were flanked by weathered, muddy paleosols of the lowstand exposure surface (c.f. "Oxidized facies" in Goodbred and Kuehl (2000); Fig. 5A; Table 1). By ~11,000 yr BP, rising sea level began to intersect the lowstand surface within the basin, leading to sediment trapping and the initiation of delta growth.

Along the Brahmaputra-Jamuna valley, a drilling project undertaken in 1976 to assess the feasibility of constructing the Jamuna Multipurpose Bridge identified a boulder and cobble layer at about 60-70 m depth below sea level at the site of the present-day bridge in north-central Bangladesh (JICA, 1976). The cobble layer is interpreted as the latest Pleistocene basal unit of the alluvial plains that form a veneer over the LPSL surface that was incised during the LGM when rivers worldwide were incising into their substrates.

Brahmaputra Avulsion and Migration History

A river avulsion is the natural process responsible for moving water discharge from one established channel to a new channel on the floodplain of the parent channel (Slingerland and Smith, 2004). Approximately 200 years ago, the Brahmaputra avulsed near the village of Dewanganj (or Dewangange) (Fig. 5) from the "Burrampooter" or Old Brahmaputra course to the channel the river occupies today, the Brahmaputra-Jamuna River. The cause and the duration of the avulsion that led to the occupation of the Brahmaputra-Jamuna remain unclear. Prominent explanations for this major avulsion include gradual tectonic basin tilting (see e.g., Kim et al., 2010), structural control due to faulting (Coleman, 1969), or in response to an avulsion in the upstream Tista River (Morgan and McIntire, 1959).

Sarker et al. (2003) report that the river still occupied the Old Brahmaputra course in 1770, but by the early 1800s it had switched its course to occupy the present Brahmaputra-Jamuna channel. Best et al. (2007) present historical evidence that suggests the avulsion occurred between 1776 and 1850 and that the Brahmaputra-Jamuna has continued to migrate westward since changing course (Fig. 5). Bristow (1999) suggests that the river avulsed

between 1830 and 1860; based primarily on the maps shown in Fig. 5, Bristow deduces that the avulsion was more likely to have been a gradual result of bank erosion rather than a catastrophic avulsion event because the 1828 and 1843 maps show flow in both the old and new channels of the Brahmaputra, where no flow was present in the 1776 map.

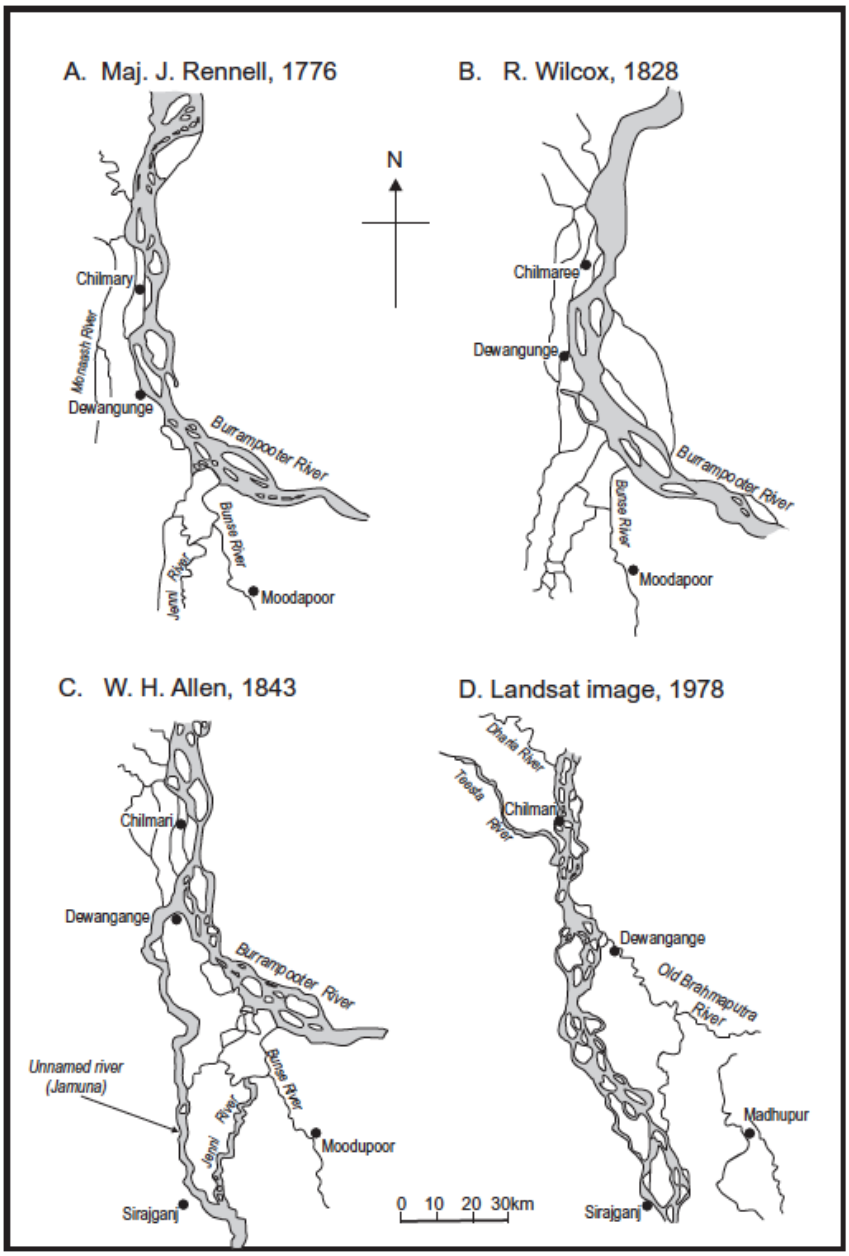

Figure 5: Historical maps of the Brahmaputra River from 1776 - 1978. From Best et al., 2007.

According to Sarker, in the early 1800s the Brahmaputra-Jamuna maintained a largely meandering planform, but the river has since evolved into its current braided planform. However, the Brahmaputra-Jamuna planform is highly variable along the length of the river, and a survey of old maps and recent satellite images suggest that the channel has fluctuated between meandering and braided over the last few decades (Best et al., 2007). Using the historical maps outlined by Best et al. (2007), the 1800s course change was a partial avulsion, wherein only a fraction of the discharge shifts to a new channel (c.f., Slingerland and Smith; 2002). This partial avulsion resulted in the Old Brahmaputra channel becoming a small distributary of the Brahmaputra-Jamuna.

Such “partial avulsion” behavior may be typical of river course changes in the Bengal basin, because large river discharge and high local rainfall are effective at maintaining distributary channels for relatively long periods of time. Such a pattern of prolonged “partial” avulsions may also complicate how avulsion and course changes are recorded in the stratigraphy. By identifying the source, lithology, and distribution of sediments preserved in the stratigraphy built by these distributary channels, we can begin to understand the avulsive behavior of the Brahmaputra and the processes that have constructed the upper Bengal delta throughout the Holocene.

CHAPTER II

METHODS

Fieldwork

Site Selection

Motivated by the historic diversion of the Brahmaputra River, Transect A borehole sites were selected to capture the valley-wide stratigraphy of both the Jamuna and Old Brahmaputra valleys downstream of the avulsion node at Dewanganj, the uplands that flank these valleys, and the delta boundary with the Shillong Anticline (annotated DEMs with transect borehole locations are given in Fig. 1 and App. A). Transect A comprises 41 boreholes spaced approximately 3 km apart over a 120 km distance, beginning near the city of Bogra and ending at the base of the Shillong Anticline. Preliminary sites were chosen using Google Earth software with some local adjustment after groundtruthing to capture prominent geomorphic features, including the eastern extent of the Barind Tract and the uplands near the city of Jamulpur.

Drilling Method and Sample Collection

The local fulcrum-and-lever tubewell drilling method was used to bring samples to the surface for collection. For this drilling method, a small water pit is dug around the borehole site for the drill fluid, and cow manure is added for buoyancy and viscosity. The fulcrum is constructed from bamboo poles with another bamboo pole as the lever (Fig. 6A). A 3 m section of PVC piping with a 5 cm diameter is then attached to the lever. One driller covers the top of the piping with his or her hand to serve as a check valve, while several others use the lever to repeatedly lift and drop the drill string. Each time the drill string is lifted, the hand valve holds suction to lift the drill fluid and sediment up with the pipe; as the raised drill pipe is dropped, the fluid and sediment, or 'wash' sample, are expelled out of the annulus and collected in a bowl. The drillers keep a measure of the borehole depth by tracking the number of 3 m sections of piping that have been attached.

Samples were collected from the drilling cuttings of Transect A at 1.5 m depth intervals, and identified according to the borehole number and depth of the sample. For example, a

sample named BNGA03102 refers to Transect A (“BNGA”), at 31 km from the start of the transect (“031”), and collected at a depth 2 m below ground surface (“02”). Half-meter increments are rounded to the nearest integer. At the time of sampling, drill fluid is decanted from the sediment, and grain size, color, and presence of gravel and/or organic material are determined in hand sample and recorded. Samples are stored in Whirl-paks for laboratory analyses.

Figure 6: (A) Fulcrum-and-lever drilling method. (B) Drill fluid being decanted off sediment. (C) Bagged samples after color and grain size description.

The drilling process and fluid flow is sufficiently competent to extract gravel, wood, and soil concretions up to the full 5-cm diameter of the piping, with the iron drill tip capable of fracturing larger clasts. Given the efficacy of this drilling method, we consider that the depth of refusal in the coring process represents a consolidated (clast supported) surface of coarse sediments that probably overlies the Pleistocene unconformity, typically identified as a lag surface of boulders and cobbles in other studies (see e.g. JICA, 1976; Goodbred and Kuehl, 2000).

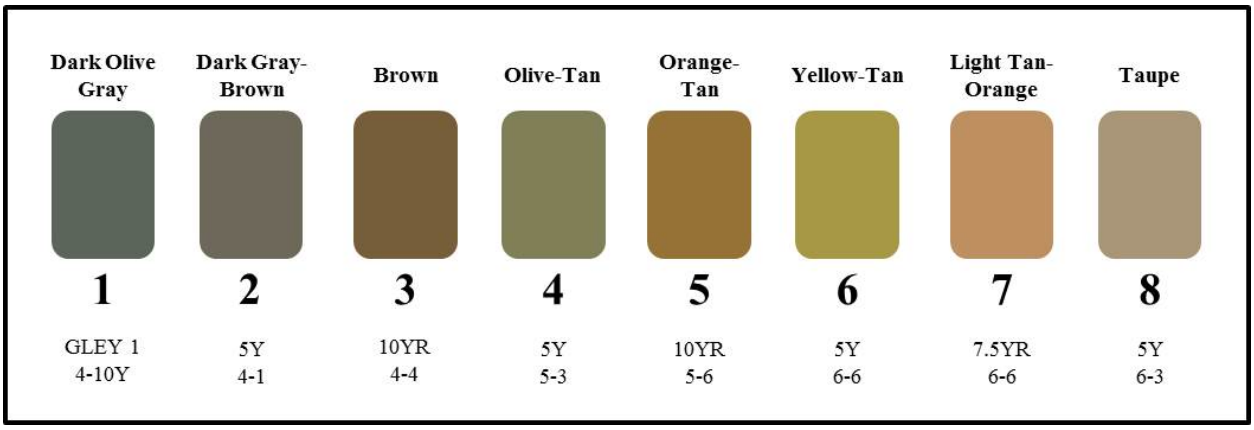

Figure 7: Color guide developed to maintain consistency in describing color of sediments. Figure provided by Christopher Tasich, Vanderbilt University.

Laboratory Analyses

Grain Size and Color Analyses

Laser particle size analysis from 0.0005-1.168 mm was performed on all samples to 20-m depth and every other sample (i.e. 3-m interval) below using a Malvern Mastersizer 2000E. Samples were sieved to remove the sediment fraction > 1.168 mm prior to laser particle size analyses (in accordance with the measurement capabilities of the instrument), and the lithology of large grains was described in hand sample and reported in Hartzog (in prep). A color guide was created and employed to maintain consistency in field descriptions (Fig. 7), and the color of each sample was noted at the time of particle size analysis. Color was used as a proxy for the degree of weathering the sediments underwent following deposition and burial, e.g. a color of "5" is interpreted as oxidized but a "3" is only mildly oxidized. In total, 953 samples were analyzed for particle size and color.

The Malvern software was used to calculate volume-weighted mode and mean grain-size diameters, as well as percentile diameters, including D_{05}, D_{16}, D_{50}, D_{84}, and D_{95}. Each of these values represents the particle diameter at a specific percentage of the total size distribution, e.g. the D_{50} is the median of the size distribution.

XRF Sample Preparation & Analyses

Geochemical analyses were performed on alternating sample of every other borehole with some analysis densification in areas of particular interest; in total 444 samples were geochemically analyzed. Sediment samples were combusted at 600°C for 48 hours and leached with acetic acid to remove detrital carbonates. Samples were then pulverized in a zirconium shatterbox. The powdered samples were compressed in a twelve-ton Carver press to form a 40 mm diameter pressed-pellet disk. Analyses targeted specifically at detecting strontium (Sr) concentrations were performed on pressed pellets using a Thermo Scientific portable XRF Analyzer. Prior to analysis, the spectrometer was calibrated using 5 known geochemical standards (NIST 2780 PP, RCR A PP, SiO_2 99.995%, NIST 2709a PP, and CCRMP TILL-4PP). A selection of 25 of these combusted, leached samples was crosschecked with ICP-MS (inductively coupled plasma mass spectrometry) results from Activation Laboratories (Actlabs).

Radiocarbon Dating

Twenty-one radiocarbon dates were obtained by the National Ocean Sciences Accelerator Mass Spectrometry Facility (NOSAMS) at the Woods Hole Oceanographic Institution from plant/wood material or from the total organic carbon (TOC) content of fine-grained sediments. These radiocarbon ages were calibrated using CALIB 6.0 software (Stuiver and Reimer, 1993) with the intcal09.14c terrestrial calibration curve, which produces a probability distribution of a sample's age. The median of the range representing twice the standard deviation (2σ), or the 95.4% confidence interval, with the highest relative area under the age probability distribution curve is reported. In the case that the reported range represented less than 90% of the area under the distribution curve, the range with the next highest area was also reported. Ages in this text are reported in calibrated sidereal years (cal BP).

CHAPTER III

RESULTS

A total of 2260 m of sediment were cored among the 41 boreholes in Transect A. Drilling depths at each site ranged from 20 to 91 m, with a mean core length of 55 m. The lithology and bulk geochemistry of these sediments reveal eight principal sedimentary facies. The spatial distribution of these facies is demonstrated in a lithostratigraphic cross-section that reveals two major fluvial paleovalleys bound by terraced interfluve or marginal structures. Five morphostratigraphic features emerge from these findings, distinguished both by characteristic surface morphology and analogous subsurface stratigraphy.

Sedimentary Analyses: Lithology and Geochemistry

Sediments recovered from Transect A boreholes are grouped into general sedimentary facies established by their similar attributes, including volume weighted mean (VWM) grain size, bulk sediment Sr concentration, occurrence of gravel, and plasticity of muds or angularity of sand grains where applicable.

Lithology

The results of 953 samples analyzed for particle size reveal a generally sandy stratigraphy with a small mud (clay + silt) fraction. The average mean grain size for all samples is 346 μm, or medium sand in the Wentworth classification. Mean grain sizes of individual samples range from 18-657 μm (silt to coarse sand), and the coarsest gravel clasts reach 5 cm, which is the diameter of the PVC drilling pipe. However, the modal grain size for Transect A is medium sand, constituting more than half (51%) of all sediments recovered during the drilling process. The frequency of other mean grain sizes is roughly evenly split between finer sediments (27% mud to fine sand) and coarser sediments (22% coarse sand to gravel) (Fig. 8A).

Downcore variations in grain size typically reflect a sand-dominated stratigraphy similar to that observed for the entire grain size dataset. The ratio of mud to sand in each borehole, as well as the proportion of samples containing gravel clasts, shows that muds typically do not

make up more than ~20% of the stratigraphy at any particular location, with exception of sites drilled in interfluve or margin settings (Fig. 9). Similarly, gravel clasts are generally present in ~10% of the sandy, matrix-dominated stratigraphy (Fig. 9).

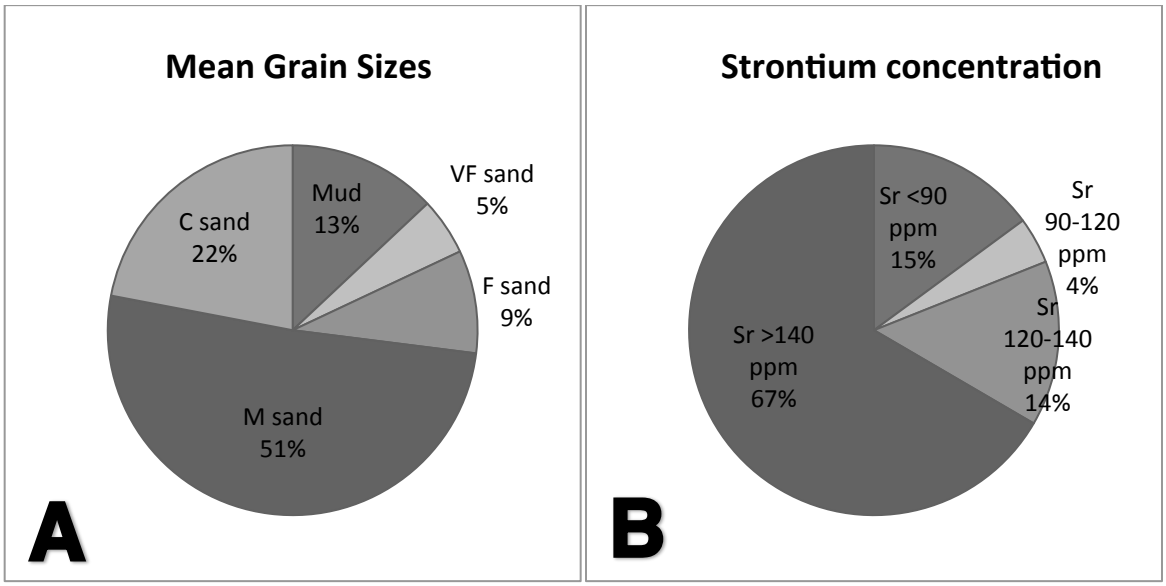

Figure 8: Percent frequency distributions for (A) Mean grain size and (B) Sr concentration distributions of all samples analyzed.

The stratigraphy of most boreholes along Transect A generally fines upward; the mean grain size of the basal deposits is typically medium to coarse sand, and the mean grain size of the near-surface deposits is mud to very fine sand in the interfluve margins and fine or medium sand in the valleys (Fig. 10). Coarse sand and gravel are rarely found shallower than 10-20 m depth. Similarly, mud is not typically preserved below the upper 10-20 m of the stratigraphy, except in the northeastern margin of the transect (Fig. 1; BNGA110-123).

In general, the sands of Transect A are well sorted, rounded, gray to gray-brown in color, and composed primarily of quartz and feldspar with abundant micas and heavy minerals. However, there is a distinctive sand lithology along the northeastern margin of the transect that is comprised of poorly sorted, angular, quartz-rich sands stained with orange-colored oxidation. The muds recovered along Transect A vary widely in color, from gray to orange to olive to nearly black. These fine sediments also have varying degrees of plasticity, which is useful in making lithological distinctions in thick or laterally extensive units of fine-grained sediments. Like the

muds, gravels of Transect A also vary in color and size and are typically intermixed with sands rather than occurring as distinct clast-supported gravel beds (Fig. 10).

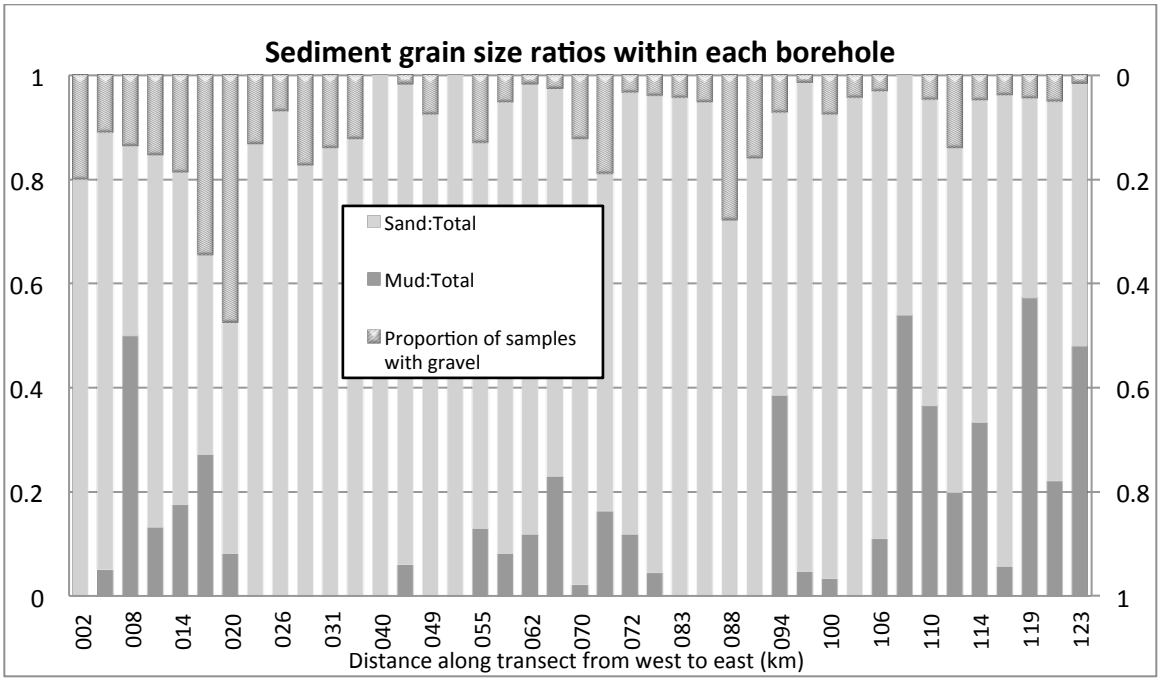

Figure 9: Fraction of mud and sand in each borehole with the proportion of samples also containing gravel clasts.

Geochemistry

XRF geochemical analyses of 392 samples reveal populations of sediment across Transect A that share similar Sr concentrations, which has been established as a regionally useful indicator of sediment provenance (e.g., Singh and France-Lanord, 2002). Four general populations of sediment emerge from the distribution of Sr concentrations (Fig. 11), including a low-Sr group <90 ppm, lower (90-120 ppm) and upper (120-140 ppm) intermediate-Sr groups, and a high-Sr group (>140 ppm). By comparison, 67% of all measured samples yielded Sr concentration values >140 ppm (high-Sr group), with the remaining samples split among the low-Sr (15%), lower (4%) and upper (14%) intermediate-Sr groups (Fig. 8B). A thorough discussion of these geochemical data and relevant background information is given in Hartzog (in prep). The general lithologic and geochemical attributes described above define unique sedimentary facies within the stratigraphy recovered along Transect A.

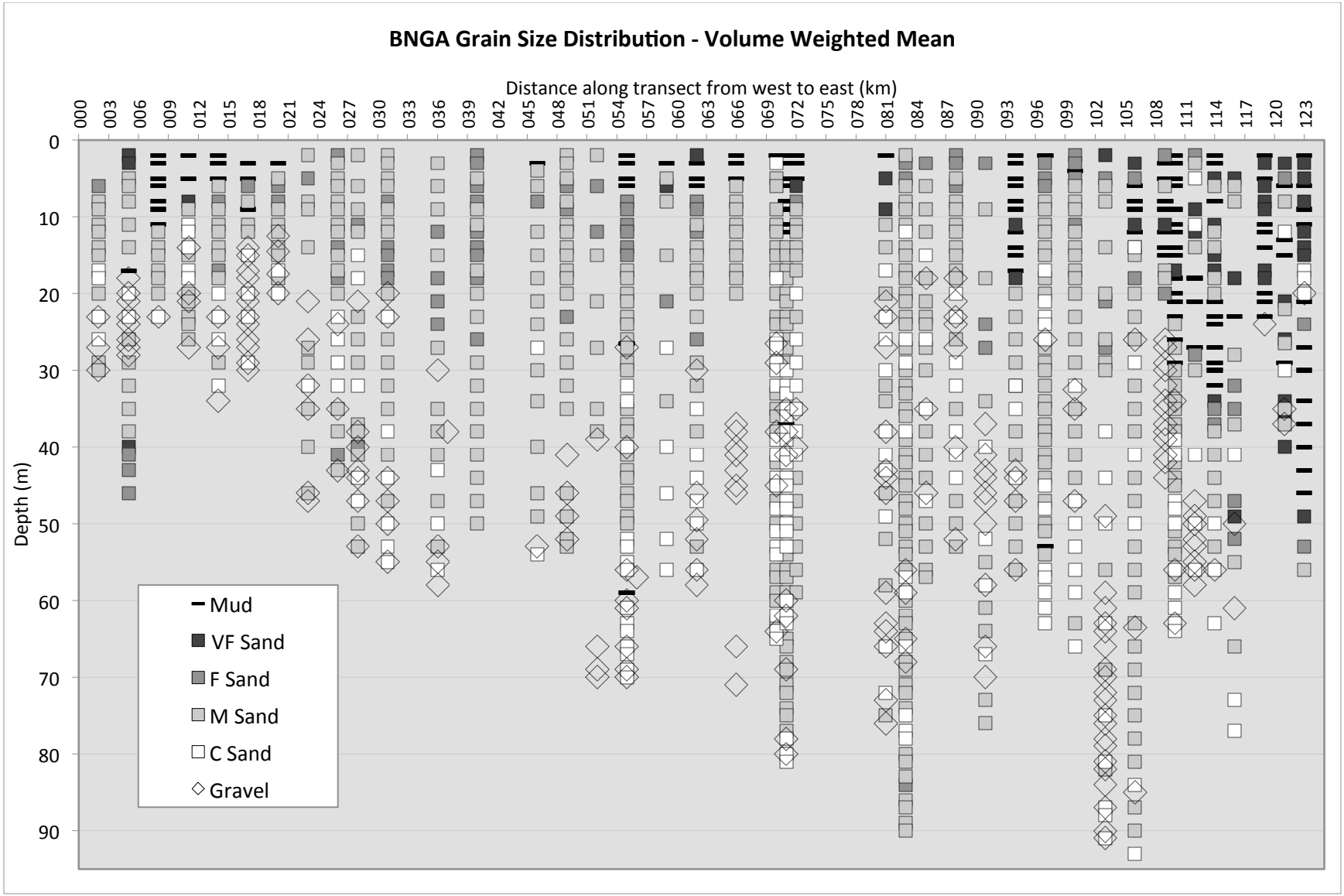

Figure 10: Grain size distribution of Transect A sediments based on the volume-weighted mean particle size of the sieved portion of each sample. Mud is defined here as 0-62.5 μm, very fine sands are 62.5-125 μm, fine sands are 125-250 μm, medium sands are 250-500 μm, and coarse sands are 500-1000 μm.

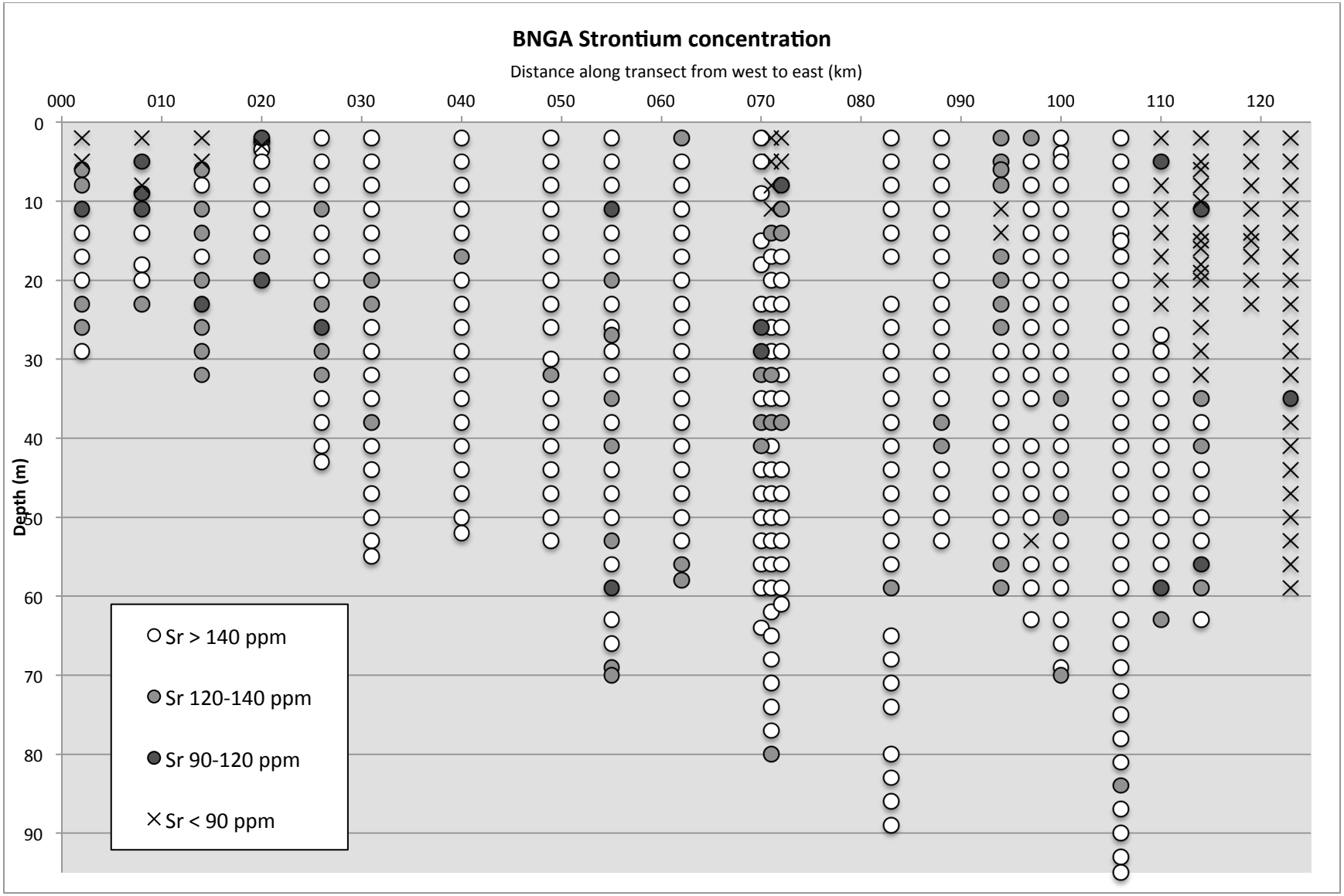

Figure 11: Sr concentrations in Transect A.

Sediment Age Constraints

Twenty-one radiocarbon dates were used to constrain the depositional history of the stratigraphy. These results are given in Table 2. We have considered the specific limitations of this dating method when interpreting the depositional periods of these facies. For example, a result of “>modern” is assumed to be modern organic material that was mixed into the sample during the drilling process; these ages are therefore not used to create the chronostratigraphy of Transect A. Two of the samples, BNGA11018 and BNGA12356, were analyzed for TOC and returned ages only slightly younger than the detection limit of the method (>48,000 yr BP), and we assume that these samples are radiocarbon-dead.

Given these considerations, the depositional period for the Basinal Mud facies, for example, began before the Holocene as is evident from 3 Basinal Mud samples with radiocarbon ages of >48,000 yr BP; we assume deposition continues to the present because the Basinal Mud facies is found at the surface of Transect A. Likewise, deposition of the Shillong Alluvium facies also began before the Holocene as it underlies sediments dated >48,000 yr BP, but because this facies is not found at the surface of the transect, we assume that deposition has occurred recently but is not presently active. This line of reasoning was used to determine the depositional period for each of the six facies; these are listed in Table 2.

Table 2: Calibrated radiocarbon ages for samples in Transect A.

Sample	Facies	^{14}C age yr BP	95.4% (2σ) median of cal age range	relative area under distribution	95.4% (2σ) median of cal age range	relative area under distribution
BNGA00823-24	Medium Sand	>modern				
BNGA02314	Medium Sand	>modern				
BNGA02346	Medium Sand	>modern				
BNGA02829	Medium Sand	>modern				
BNGA02840	Fine Sand	7020±35	cal BP 7863	0.987		
BNGA03615	Medium Sand	390±25	cal BP 468	0.793	cal BP 343	0.192
BNGA03638	Medium Sand	7980±45	cal BP 8848	0.964		
BNGA05559	Overbank Mud	5800±30	cal BP 6586	1		
BNGA08134	Medium Sand	>48000				
BNGA08521	Medium Sand	8580±45	cal BP 9558	0.986		
BNGA09127	Fine Sand	405±25	cal BP 474	0.902		
BNGA09735	Medium Sand	5980±45	cal BP 6829	0.983		
BNGA09739	Medium Sand	5930±35	cal BP 6736	0.901		
BNGA10912	Overbank Mud	695±25	cal BP 665	1		
BNGA11008	Basinal Mud	4130±30	cal BP 4648	0.665	cal BP 4786	0.28
BNGA11018	Basinal Mud	41300±480	cal BP 44937	1		
BNGA11211	Shillong Alluvium	5510±35	cal BP 6337	0.961		
BNGA11456	Medium Sand	>48000				
BNGA11463	Medium Sand	>modern				
BNGA12129	Basinal Mud	>48000				
BNGA12356	Basinal Mud	43200±730	cal BP 46609	1		

Sedimentary Facies Descriptions

Lithological, geochemical, and radiocarbon results define five major sedimentary facies from Transect A, three of which are further subdivided based relative age and weathering characteristics, resulting in eight distinct sedimentary facies. These include Fluvial Overbank Muds, Basinal Muds, and Braidbelt Sands, each further distinguished as Holocene or Pleistocene age, plus the Shillong Alluvium and Pleistocene Lowstand Gravel facies (Table 3; Fig. 12).

Fluvial Overbank Muds

Sediments of this facies are distinguished as soft brown silts (20-80 μm) that occur as relatively thin (5-10 m), shallow (<10 m) deposits along the margins of the principal river valleys

(Table 3). An exception is the Overbank Mud facies in BNGA094, which is ~20 m thick but appears to comprise several stacked units of this same facies. Fluvial Overbank Muds are also present less frequently as thin (~1 m) isolated deposits at depths to 60 m within a principally sandy stratigraphy.

Within the Overbank Mud facies there are two sub-units that can be consistently distinguished by their rheological properties, varying between soft, deformable muds and those that are much stiffer and extruded from the well as undeformed, cylindrical plugs of sediment. Based on radiocarbon dates, the soft, highly plastic muds typically correspond with strata deposited during the Holocene, whereas the undeformed, low-plasticity muds were deposited at least 48,000 yr BP, i.e. these muds contain radiocarbon-dead organic material. The low-plasticity muds are part of a thick paleosol that typically has a gray soil matrix (i.e. redox depletions) with prominent orange mottling associated with iron oxide formation. This paleosol generally occurs as a unit thicker than 10 m, although thin beds of these stiff muds may be found locally along the transect. These paleosol sediments weathered at the latest Pleistocene land surface that was exposed until post-deglaciation sedimentation and burial.

The Holocene and Pleistocene Overbank Muds share similar grain sizes, but they are, in general, geochemically distinct. The mean grain size of Holocene Overbank Muds is 44 μm, and strontium concentrations in this sub-facies are generally >140 ppm, although measurements in the 120-140 ppm range are not uncommon. In the westernmost portion of the transect, Sr concentrations as low as 90 ppm were measured in the Holocene sub-facies. Similarly, the mean grain size of Pleistocene Overbank Muds is 37 μm; however, strontium concentrations in the Pleistocene sub-facies are generally lower than those in the Holocene sub-facies at <120 ppm, although Sr concentrations up to 140 ppm were measured in borehole 094.

Basinal Muds

A second fine-grained facies, the Basinal Muds, consist of muddy to sandy silts (18-99 μm) with a variety of colors and oxidation states (e.g., Fig. 7C). These muds can be differentiated from the Fluvial Overbank Muds by their low Sr concentration, color variability, and unit thickness. Strontium concentrations for the Basinal Muds are almost exclusively <90 ppm, making it the only facies along Transect A the have such consistently low Sr values. The sediments having these facies characteristics are also spatially contiguous and found only in the easternmost portion of Transect A and at the northwestern margin of the Sylhet Basin.

The Basinal Muds are further distinguished into Holocene and Pleistocene facies based on radiocarbon ages and their rheology (i.e., highly-plastic Holocene muds vs. low-plasticity Pleistocene paleosols). Both Basinal Mud facies have a mean grain size ~50 μm, but Holocene-age units are generally thinner (~10 m) and shallower (<30 m) than the Pleistocene deposits that are ~10-30 m thick and deeper in the stratigraphy (10-60 m). Together these two sub-facies define a lithologically and morphologically unique wedge-shaped deposit that thickens towards the Shillong Anticline (BNGA109-123).

Braidbelt Sands

Among the coarse sandy facies, the Braidbelt Sands are the most abundant and widespread. These deposits comprise clean fine-to-coarse sands (76-657 μm) with some feldspars and abundant micas and heavy minerals. The sands are generally gray or gray-brown in color but may be mildly oxidized to slight orange or tan at depth in some areas. The Braidbelt Sands also have characteristically high Sr concentrations, typically >140 ppm but with some locally lower values (120-140 ppm).

As with the Overbank and Basinal Muds, the Braidbelt Sands are divided into Holocene and Pleistocene sub-facies. However, these sandy deposits do not preserve well-defined paleosols, as the mud facies do, and so distinguishing Holocene and Pleistocene aged Braidbelt Sands is less straightforward. In many instances, the Pleistocene-Holocene distinction was readily defined by radiocarbon dates, allowing us to identify several lithological attributes typically associated with the Pleistocene-age deposits. These include the higher occurrence of gravel and dried-mud clasts in Pleistocene sands and their coarser mean grain size (447 μm vs. 378 μm).

Along the transect, Holocene-age Braidbelt Sands constitute the fill sediments within the lowstand valleys, occurring as deep as 70 m in the Brahmaputra-Jamuna valley and 80 m in the Old Brahmaputra valley. Most of the Pleistocene Braidbelt Sands underlie Pleistocene-aged Overbank Mud or Basinal Mud deposits.

Shillong Alluvium

In contrast to the well-rounded, sorted Braidbelt Sands, the Shillong Alluvium consists of angular, poorly sorted, often coarse, sand and granules. The size fraction >1.1 mm often

contributes >50% of the facies by weight, and the portion sieved for laser diffraction size analysis (<1.1 mm) yielded a mean grain size of 330 μm with a range from 102-588 μm. These sands occur locally in units <10 m thick and are exclusively found within the wedge-shaped deposit of Basinal Muds in the easternmost transect. Samples in this distinctive facies were analyzed geochemically, and ranged from 71-87 ppm Sr. The Shillong Alluvium occurs above and below the Holocene-Pleistocene boundary, but without distinct variation and therefore not subdivided by age.

Pleistocene Gravel

The Pleistocene Gravel facies is composed of generally rounded gravels of mixed Himalayan lithology. These clasts were not analyzed for bulk geochemistry; however, Sr measurements of the matrix sediments supporting these clasts range from 105 to 184 ppm with an average of 144 ppm. The gravels recovered at the base of the BNGA011-062, measuring up to 50.8 mm in diameter, which is the maximum diameter of the drill core, are part of the top of a thick (10 m) lowstand gravel unit that underlies the Brahmaputra-Jamuna valley (Umitsu, 1993). The gravel unit coarsens with depth, reaching cobble to boulder-sized clasts, as revealed through geotechnical drilling in the feasibility study for the Jamuna Bridge by the Japan International (JICA, 1976). We are also able to corroborate that the gravels and depth of refusal for our cores in this area coincide with this lowstand gravel surface based on results of multi-channel seismic data collected during a river survey in 2011. In these seismic data the gravel unit is revealed as a prominent, and largely contiguous, seismic reflector along the length of the Brahmaputra-Jamuna valley. The velocity-migrated depth of the reflector places it at the same 60-70 m depth of refusal as our corresponding Transect A cores (Fig. 13).

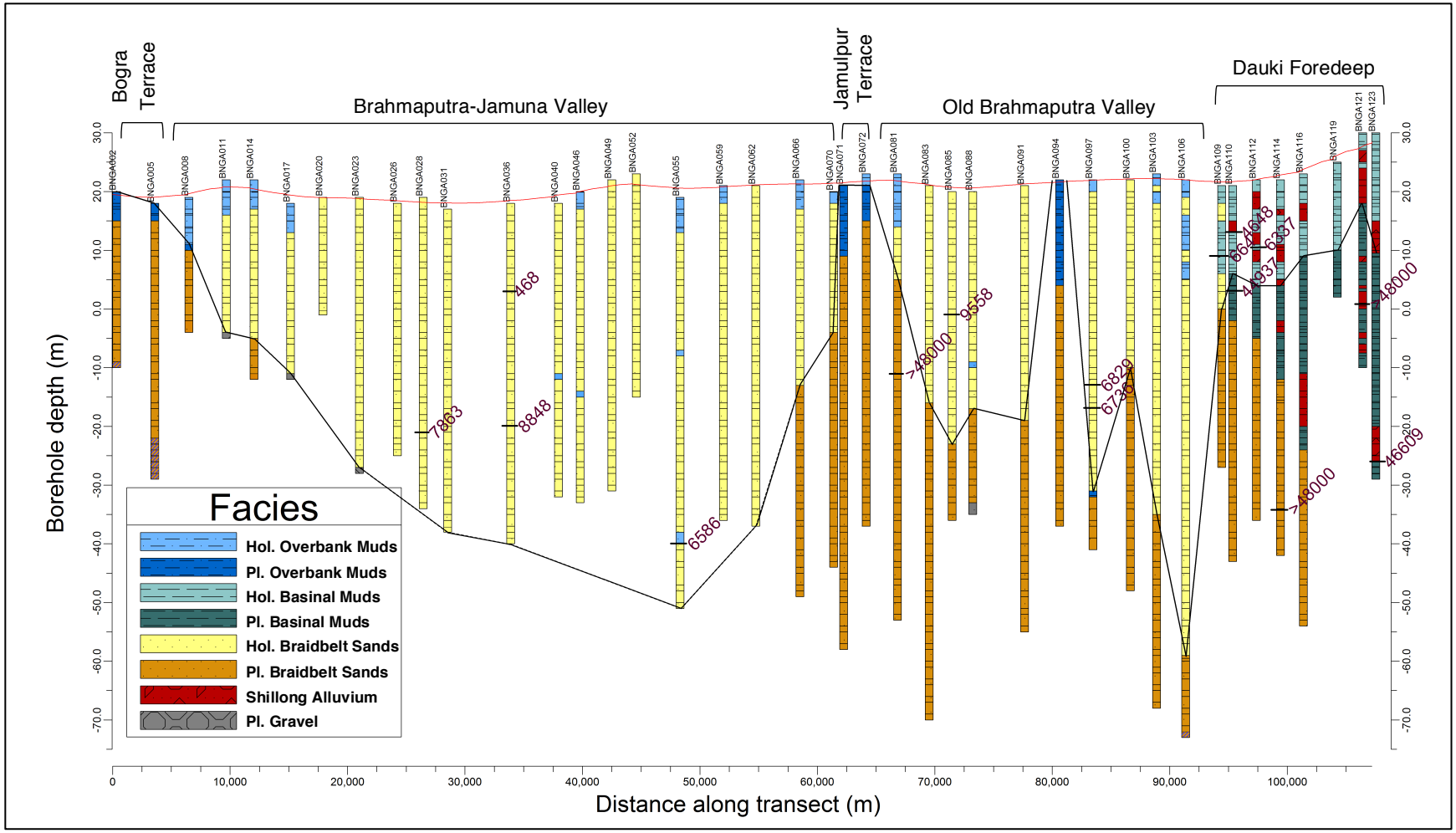

Figure 12: Facies distribution of Transect A. The black line shows the Pleistocene-Holocene stratigraphic contact and defines the morphologies of the Brahmaputra-Jamuna and Old Brahmaputra valleys.

Table 3: Sedimentary facies of Transect A.

Facies	Lithology	Sr concentration	Spatial distribution	Thickness	Depth to top	Period of deposition	Interpretation
Holocene Fluvial Overbank Muds	Thin silt deposits	Typically >140 ppm but 120-140 ppm not uncommon; occasionally ~90 ppm in Bogra	Shallow subsurface at valley margins; occasional localized deposit at depth	Typically ~5 m; localized deposits are ~1 m at depth	Typically surface to <10 m at valley margins; few locally at depth	~10,000 BP to present	Modern and preserved overbank deposits
Pleistocene Fluvial Overbank Muds	Generally stiff silts often underlain by silts; typically gray matrix with orange mottling	Generally <120 ppm; up to 140 ppm in core 094	Prevalent in shallow subsurface of valley margins and upper ~20 m of core 094	1-20 m; typically ~5-10 m	Surface to ~55 m	Pre-Holocene (Late Pleistocene)	Overbank deposits with well-developed paleosols
Holocene Basinal Muds	Soft silts of varying color	Consistently <90 ppm	Locally in cores 109-123	Generally 15-20 m, with interspersed sands in some cores	0-20 m	Holocene	Dauki foredeep deposits
Pleistocene Basinal Muds	Generally stiff silts; stiffness decreases with depth below weathering horizon		Locally in cores 110-123	Up to 40 m with interspersed sands	10-60 m	Pleistocene	
Holocene Braidbelt Sands	Clean, quartz-rich very fine to coarse sands; typically gray or gray-brown in color; gravel often present	Generally >140 ppm; 120-140 ppm not uncommon; occasionally as low as 90 ppm	Widespread in paleovalleys	Up to 80 m thick in deepest parts of valleys	0-80 m	Holocene	Alluvial deposits of the Brahmaputra (valley fill)
Pleistocene Braidbelt Sands			Widespread below paleovalleys, mud-capped features, and Dauki foredeep	Up to 80 m thick in longest boreholes	15-95 m	Pre-Holocene (Late Pleistocene)	Alluvial deposits of paleo-Brahmaputra rivers
Shillong Alluvium	Angular and poorly sorted but generally coarse quartz sands and granules	<90 ppm	Locally in cores 109-123 (northwestern margin of Sylhet Basin)	<10 m	2-55 m	Pre-Holocene to recent	Shillong-sourced ephemeral stream deposits
Pleistocene Gravel	Rounded to sub-angular lithic material up to 50.8 mm diameter	Not analyzed	Occur below western half of transect at base of Jamuna paleovalley	Unknown	20-50 m	Pre-Holocene (Late Pleistocene)	Lag deposit from LGM valley incision

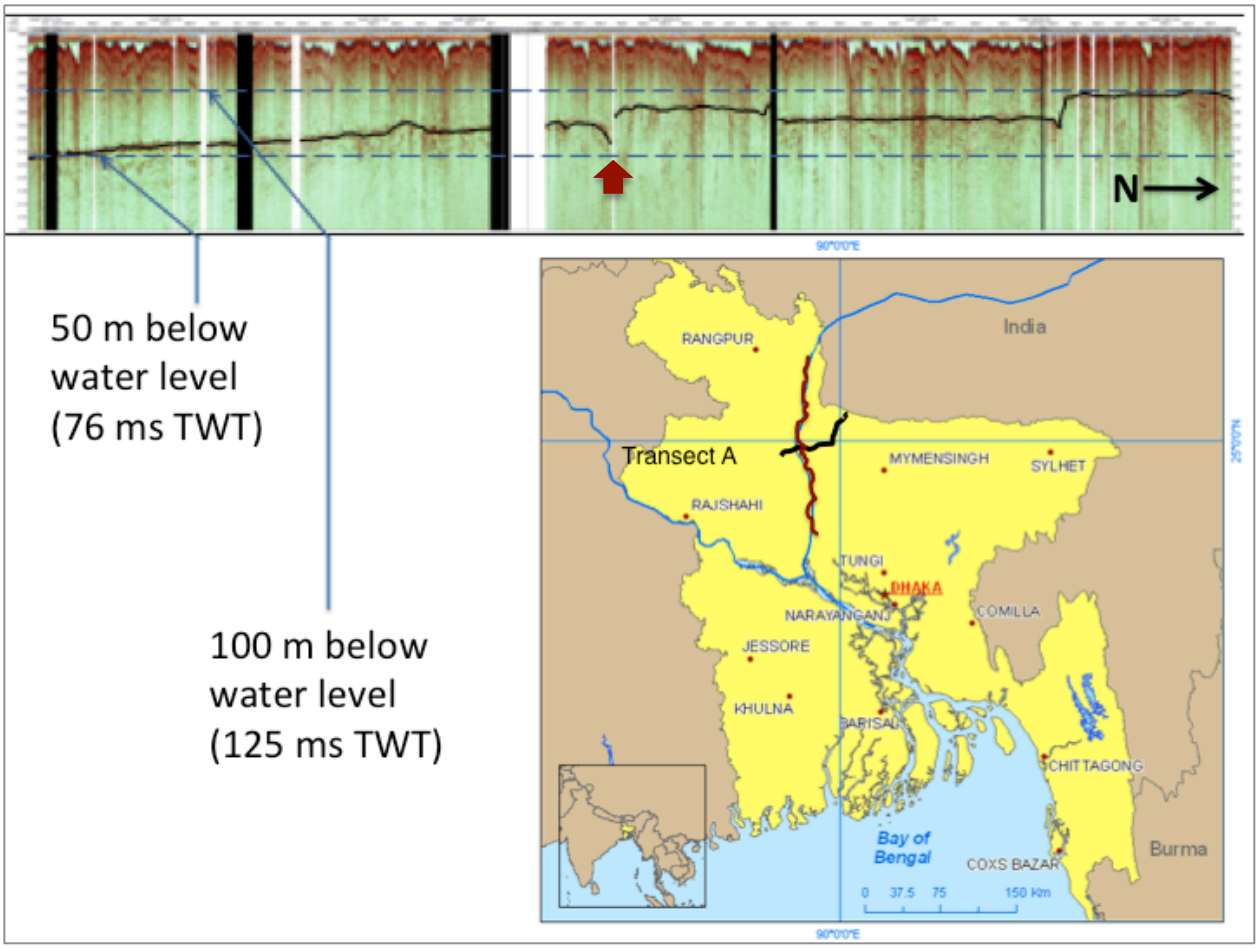

Figure 13: Above - 2011 seismic line data along Brahmaputra-Jamuna River with traced gravel reflector (in black); red arrow shows approximate location where seismic line crosses Transect A. Below - location of the seismic line (in red) crossing Transect A (in black). Seismic data courtesy of Volkhard Speiß and Tillman Schwenk, Bremen University.

Facies Distribution in Space and Time

The spatial and temporal components of the Transect A facies are equally as important as the physical properties. Five morphological subdivisions are apparent from Shuttle Radar Topography Mission (SRTM) topography and satellite imagery of the study area and largely correspond with the underlying stratigraphy. In addition to this surface-to-stratigraphy spatial analysis, the geochronology of Transect A is constructed using 21 radiocarbon ages that generalize the periods of deposition for each facies.

Morphology-Stratigraphy Relationship

Transect A crosses five distinct surface morphologies in the upper Bengal Delta. From west to east, these are the Bogra Terrace (the easternmost extent of the *Barind Tract*), the Brahmaputra-Jamuna Valley (*Flood Plain*), the Jamulpur Terrace (unmapped, just north of the *Madhupur Terrace*), the Old Brahmaputra Valleys (*Flood Plain*), and the Dauki Foredeep (*Meghalaya Foothills*) (Fig. 3; Fig. 14). Here we discuss the stratigraphy associated with these surficial geomorphic expressions.

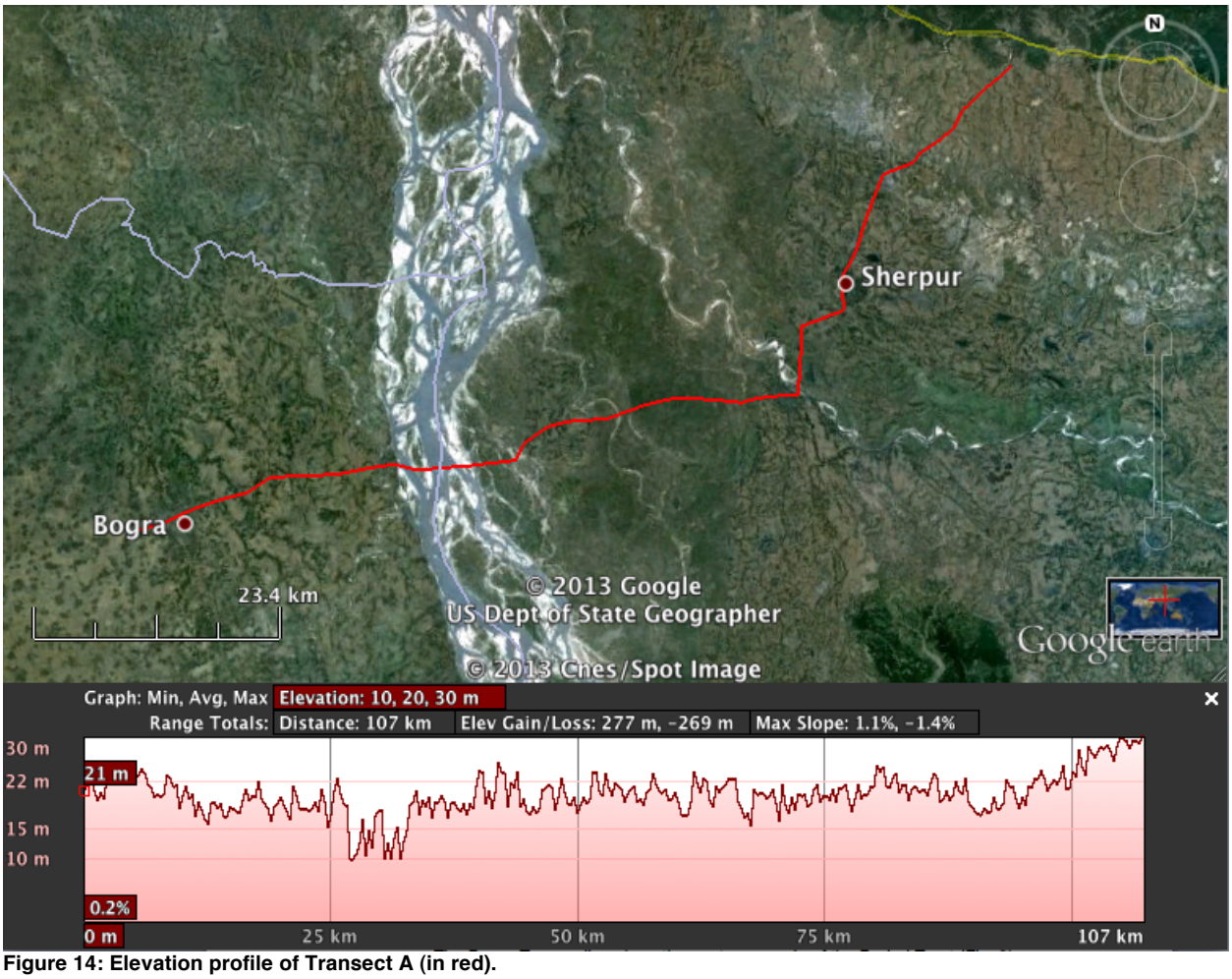

Figure 14: Elevation profile of Transect A (in red).

Bogra Terrace

The Bogra Terrace lies along the eastern margin of the Barind Tract (Fig. 3). Located at the western edge of Transect A, the terrace deposit extends from BNGA002 to BNGA008, and lies 5-10 m higher than the adjacent Holocene floodplain (Fig. 14). This morpho-stratigraphic unit is composed of Pleistocene Overbank Muds and particularly gravel-rich Braidbelt Sands with a thin cap of Holocene Overbank Muds on BNGA008. The abundance of gravels in this unit is likely due to the proximity to the Tista River megafan, which Hartzog (in prep) suggests is the source for the gravel-sized sediments in the Holocene valleys of Transect A.

Bogra Terrace cores range from 25-45 m deep, which is shallow in comparison with the whole transect mean core length of 55 m. This shallow depth of refusal is a result of the terrace lithology, which is up to 20% gravel (BNGA002) and 50% mud (BNGA008), sediments that are more difficult to drill through than clean sands.

Bogra Terrace sediments above 15 m depth populate the low-Sr (<90 ppm) or lower intermediate-Sr (90-120 ppm) groups, comparable to shallow sediments of the Jamulpur Terrace (Fig. 11). Sediments below 15 m, however, typically populate the upper intermediate-Sr (>120 ppm) or high-Sr (>140 ppm) groups, which is similar to, if not slightly lower than, the high-Sr sediment majority in Transect A.

Brahmaputra-Jamuna Valley

The Brahmaputra-Jamuna River Valley spans nearly 60 km from the Bogra Terrace to the Jamulpur Terrace from BNGA011 to BNGA070 (Fig. 12). The grain size of the Brahmaputra-Jamuna Valley generally fines upward with the shallow stratigraphy of this unit generally comprising a thin (< 5m) cap of Overbank Muds overlying thick (20-60 m) successions of Holocene Braidbelt Sands. Braidbelt Sands comprise 93% of the lithology, with only highly localized Holocene Overbank Muds preserved at depths up to 55 m.

Brahmaputra-Jamuna Valley sediments are almost solely high-Sr (>140 ppm), with few samples yielding upper immediate-Sr (120-140 ppm) signatures. This geochemical homogeneity suggests that the main Brahmaputra River has occupied this valley exclusively, i.e. no other rivers have avulsed into this valley, for much of the

Holocene, limiting the amount of mud preserved in this upper portion of the delta.

Jamulpur Terrace

The Jamulpur Terrace, about 12 km northwest of the northern margin of the Madhupur Tract, is roughly 22 m in elevation, which is similar to the Bogra Terrace, and marks the point of bifurcation between the 2 major fluvial valleys of Transect A. This unit consists of a 10 m thick cap of Pleistocene Overbank Muds overlying Pleistocene Braidbelt Sands. BNGA071 and 072 are completely contained within this unit, and BNGA070 and 081 partially underlie the Jamulpur Terrace, i.e. the lower halves of these cores have Jamulpur stratigraphy, whereas the upper halves are Holocene Braidbelt stratigraphy.

Overbank Muds capping the Jamulpur Terrace and the Braidbelt Sands below the surface are both oxidized, suggesting Pleistocene deposition, and a radiocarbon date of >48000 cal yr BP at 34 m depth in BNGA081 further corroborates this. Sediments here, however, are not as deeply weathered as those found on the Madhupur Tract, which is widely accepted as a Pleistocene landform (e.g. Rashid et al., 2006).

Old Brahmaputra Valley

The Old Brahmaputra Valley spans 28 km (BNGA081-109) and much of the eastern portion of Transect A. It is situated between the Pleistocene Jamulpur terrace and the lithologically distinct Dauki Foredeep mud-wedge. The abrupt changes in stratigraphy at the marginal features of the Old Brahmaputra Valley indicate sharply bound valley walls. The broader valley feature actually comprises two smaller valleys, bifurcated by a remnant of the Jamulpur Terrace (BNGA094). Each of these Old Brahmaputra sub-valleys is only the width of the modern Brahmaputra braidbelt (10-15 km).

The Old Brahmaputra Valley unit is composed of Holocene Braidbelt Sands in the shallow subsurface and Pleistocene Braidbelt Sands in the deeper subsurface with localized deposits of Holocene Overbank Muds at the margins and Pleistocene Overbank Muds at depth and in borehole 094. The sediments of this valley are similar to those in the Brahmaputra-Jamuna Valley, but the depth to Pleistocene stratigraphy is

more shallow in the western sub-valley and deeper in the eastern sub-valley. Additionally, the width of each sub-valley is only a third that of the Brahmaputra-Jamuna Valley.

Dauki Foredeep

The Dauki Foredeep basin is a sloping surface that lies up to 10 m higher than the adjacent Old Brahmaputra sub-valleys. The basin extends 13 km south from the outcropping Neogene uplands of the Garo Hills (BNGA109 to BNGA123). This unit contains Holocene and Pleistocene Basinal Muds that form a wedge-like shape, which pinches out to the southwest and opens to the northeast. The coarse, angular Shillong Alluvium is interspersed throughout this mud-wedge and is readily linked with the small alluvial stream draining the Garo hills. These small rivers build local channel-levee deposits across the foredeep and appear as thin gravelly sand deposits within the much thicker Basinal Muds, which are underlain by Pleistocene Braidbelt Sands.

The Dauki Foredeep lithology is distinct from every other part of the transect. Basinal Muds in both the Pleistocene and Holocene portions of the stratigraphy vary widely in color, from oxidized to reduced, and nearly every sample measured <90 ppm strontium concentration. The Dauki Foredeep stratigraphy ends abruptly at the eastern margin of the Old Brahmaputra Valley between BNGA109 and 110.

CHAPTER IV

DISCUSSION

In defining the LPSL surface in the stratigraphy of Transect A, we have identified discrete valleys that were formed by river incision during sea-level lowering in the latest Pleistocene. Here we interpret the fluvial processes that have deposited these sediments. Utilizing strontium as a geochemical indicator of sediment provenance, Hartzog (in prep) shows that the Brahmaputra River deposited the sands found in both the Brahmaputra-Jamuna and Old Brahmaputra valleys. It then follows that, in general, variations in grain size represent changes in flow dynamics at a given depositional environment rather than changes in the sediment source input. Because avulsions allow floodplain deposits to be preserved, we are able to infer the process of river abandonment where such stratigraphy exists.

Gibling (2006) compiled and characterized channel bodies and fluvial valley fills for more than 1500 rivers based on their dimensions and internal architecture, specifically the width-to-thickness (W/T) aspect ratios of these sand bodies. Fluvial processes typical of these rivers were then compared with their W/T ratios, and generalized behaviors were extrapolated for each range of aspect ratios. Here we compare the inferred fluvial processes for the Brahmaputra-Jamuna and Old Brahmaputra rivers from the W/T ratio of these valleys. Coupling the subsurface stratigraphy with each valley's morphology allows us to then broadly reconstruct the history of delta construction since the LGM.

Brahmaputra-Jamuna Valley

Stratigraphy and Morphology

The Brahmaputra-Jamuna valley is infilled almost exclusively with Holocene Braidbelt Sands deposited by the Brahmaputra-Jamuna River (Hartzog, in prep). Holocene Overbank Mud deposits are present below the shallow subsurface (below 10 m) of only 3 of the 19 boreholes drilled in this valley. In order for mud to be preserved, the channel must avulse away from the floodplain where the mud is deposited, rather than eroding into the floodplain, so a lack of preserved subsurface mud indicates a laterally mobile river and post-depositional sediment reworking. Although erosional surfaces are not preserved with our tubewell drilling method, the

general lack of mud in these stratigraphic sections, which are up to 70 m thick, is a clear indication that the Brahmaputra-Jamuna valley is composed of multistory sand bodies.

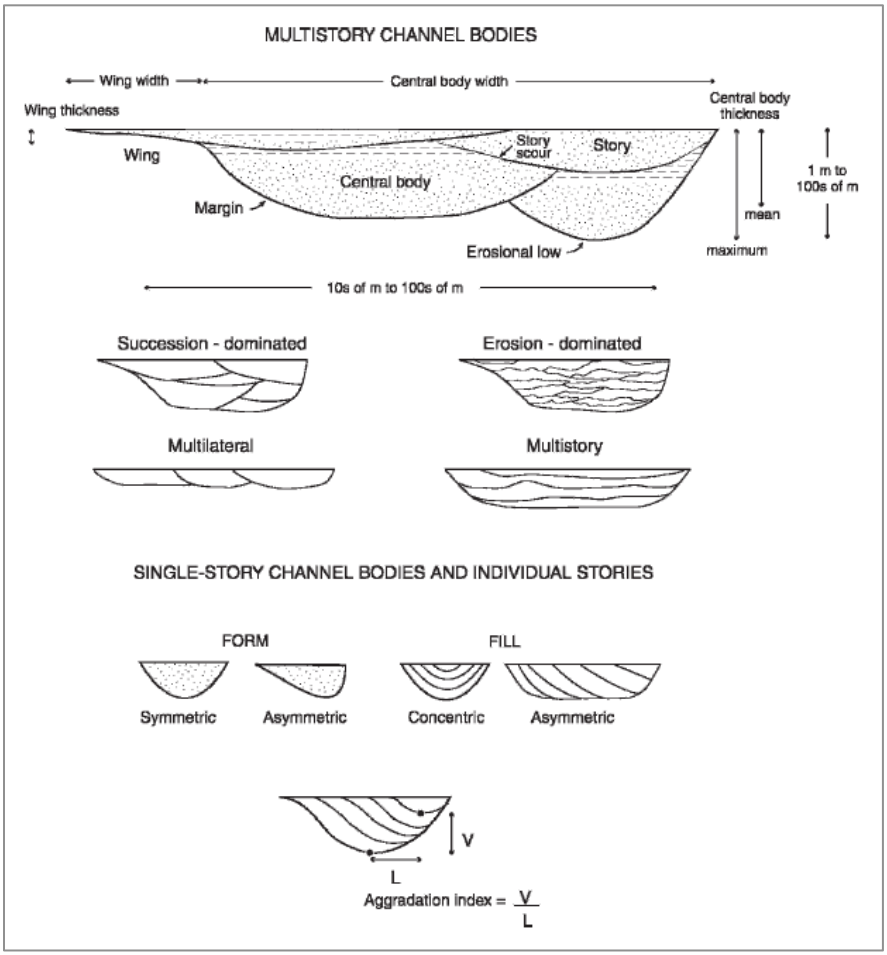

Figure 15: Multistory verses single-story channel bodies. From Gibling, 2006.

The stratigraphy of the Brahmaputra-Jamuna valley contains almost no gravels in the upper 20 m, and the modern river transports a negligible amount of gravel today. Hartzog (in prep) concludes that non-basal gravel deposits in the Brahmaputra-Jamuna valley are indicative of lateral migration of the river into the adjacent Bogra Terrace deposits that bound the valley. The abundance of gravels and the ages of the dated organic samples in this valley suggest that the lower half of the stratigraphy represents valley infilling during the early-mid Holocene, and the clean-sand upper half of the stratigraphy represents aggradation during the mid to late Holocene.

The Brahmaputra-Jamuna valley is wider than the Old Brahmaputra valley (Fig.12). The modern Brahmaputra-Jamuna braidbelt comprises boreholes BNGA028-040 and has a width of ~12 km at Transect A. This braidbelt width is small in comparison with the total valley width of ~62 km at the surface. In order for a channel to form a valley more than five times its own width, it is necessary for the braidbelt itself to be highly mobile in the lateral direction. We see further evidence of the Brahmaputra-Jamuna's lateral mobility in the winged western margin of this asymmetric valley. A valley wing is a thin channel body that is positioned on one side of a multistory body, creating an elongated morphological feature on one side of the valley at the top of the cross-section (Fig. 15). The winged portion of a multistory channel body is indicative of erosion-dominated processes.

Although the winged western wall of this valley, signified by the Pleistocene-Holocene contact, is less constrained than the eastern Jamulpur Terrace wall, it is apparent that this side of the Brahmaputra-Jamuna valley is much less vertical, i.e. it dips more shallowly, than the eastern wall. This may be a result, at least in part, of the lithology of the Barind Tract deposits, which are more friable than those of the Jamulpur Terrace. This lithological difference likely facilitates riverbank erosion of the Brahmaputra-Jamuna River into the western wall of the valley, whereas the eastern valley wall at the Jamulpur Terrace, several meters higher in elevation with a mud-cap >10 m thick, is less easily eroded into.

The morphology of the Brahmaputra-Jamuna valley is indicative of a laterally mobile river braidbelt under Gibling's (2006) dimensional classification scheme. The valley has a width to thickness ratio of 886 (where $W = 62$ km and $T_{max} = 70$ m) and is composed of stacked multistory channel bodies that fine upwards. This W/T ratio indicates that the Brahmaputra-Jamuna has maintained a braided or low-sinuosity river planform within a mobile-channel belt throughout the Holocene. Our results are consistent with this: sand and minor gravels dominate the fining-upward stratigraphy, muds are localized abandonment fills, and the modern river has a braided planform. From these attributes, we can then infer that the Brahmaputra-Jamuna accretes laterally as the result of a high rate of bank migration and avulsion periodicity (Fig. 16); i.e. when this valley is occupied by the Brahmaputra, the river is free to move laterally without avulsing into a new channel path, so there is more time between avulsions.

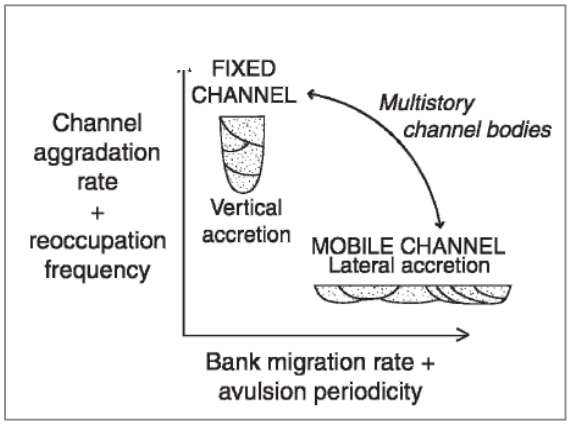

Figure 16: Conceptual model relating deposition to mobility processes in multistory river stratigraphies. From Gibling, 2006.

Old Brahmaputra Valley

Stratigraphy & Morphology

The Old Brahmaputra valley, like the Brahmaputra-Jamuna valley, is composed almost entirely of Holocene Braidbelt Sands with only 2 of 8 boreholes containing Holocene Overbank Muds below ~ 10 m. Boreholes 083 through 091 correspond to the location of the Old Brahmaputra channel. Borehole 094 is in the modern village of Sherpur. On a historical map by Rennel (1776), the location of Sherpur, or “Seer pour” is mapped, as is “Dewangunge”, the location of the avulsion node. Given the persistence of the village of Sherpur, the relatively higher elevation of borehole 094 than the adjacent boreholes and the oxidation within borehole 094, we suggest that the town of Sherpur is built upon a remnant of the Pleistocene Jamulpur Terrace that was not eroded away during lowstand incision. This remnant bifurcates the Old Brahmaputra valley into 2 sub-valleys, one to the southwest and one to the northeast of borehole 094. The Old Brahmaputra River occupied the southwestern sub-valley (henceforth referred to as sub-valley A) until the late 18th-early 19th century avulsion.

The Old Brahmaputra sub-valleys are constrained by shallow Pleistocene deposits. These sub-valleys are composed of what appear to be multistory sands (Fig. 15). However, lateral migration and sediment reworking are less apparent here than in the Brahmaputra-Jamuna valley, e.g. neither of the Old Brahmaputra sub-valleys has a winged geometry and the

valley walls are much steeper than the western wall of the Brahmaputra-Jamuna valley. This suggests that the Old Brahmaputra sub-valleys are fixed channels (Gibling, 2006).

Sub-valley A contains a single subsurface Overbank Mud deposit that overlies a sub-valley wide unit of sands with a slight orange tint. We attribute this to vadose zone weathering in the form of mild oxidation in these sands, which are situated just above the Pleistocene-Holocene boundary. This stratigraphy suggests that the Old Brahmaputra valley may remain unoccupied for long timescales after an avulsion. These Holocene Braidbelt Sands are less oxidized than Pleistocene Braidbelt Sands, such as those underlying the Jamulpur Terrace, for example. For comparison, surface sands around Mymensingh, which were deposited by the Old Brahmaputra and abruptly abandoned during the late 18th-early 19th century avulsion, have a similar degree of oxidation.

In addition to the mild oxidation present in sub-valley A, the 2 Old Brahmaputra sub-valleys have different W/T aspect ratios. Sub-valley A has a width to thickness ratio of 244 (where W = 10 km and T_{max} = 41 m), which classifies it as a delta distributary fixed channel (Gibling, 2006). Sub-valley B (the northeast sub-valley) has a width to thickness ratio of 123 (where W = 10 km and T_{max} = 81 m), which is also indicative of a delta distributary fixed channel. These W/T ratios indicate that the Old Brahmaputra has been a distributary channel of the Brahmaputra throughout the Holocene and that the incision of these valleys was primarily the result of avulsive scour (Gibling, 2006). Our results are consistent with this: sand and minor gravels dominate the fining-upward stratigraphy, muds are rare, and the modern channel has low-sinuosity. From these attributes, we can then infer that the Old Brahmaputra aggrades vertically as the result of a low rate of bank migration into the cohesive sediments that form the boundaries of these sub-valleys. The reoccupation frequency in this part of the delta is high, i.e. the river consistently reoccupies this bifurcated valley post-avulsion (Fig. 16). This rapid vertical aggradation of reoccupied channels causes the river to avulse away from this side of the valley more quickly than in the more laterally mobile Brahmaputra-Jamuna valley.

Avulsion Processes and History

The Brahmaputra-Jamuna valley, infilled with multistory channel bodies, permits a relatively high bank migration rate and avulsion periodicity and a relatively low channel aggradation rate and reoccupation frequency when compared to the Old Brahmaputra valley. The Old Brahmaputra sub-valleys, fixed channel bodies, permit higher rates of channel

aggradation and reoccupation frequencies, as well as less bank migration and a smaller avulsion periodicity than the Brahmaputra-Jamuna channel.

The antecedent topographic controls, i.e. the incised valleys and exposed upland terraces that bound the Old Brahmaputra create constrained channels. This causes the riverbed to aggrade relatively rapidly with little lateral migration. In this scenario, the river will avulse out of its valley. While it is easy to understand why the river avulses away from the Old Brahmaputra channel after rapid aggradation, it is more difficult to explain why the Brahmaputra-Jamuna River would avulse into the Old Brahmaputra valley. Given Gibling's conceptual model in conjunction with our stratigraphic evidence, we know that the Brahmaputra-Jamuna is more prone to lateral migration into the eastern extent of the Barind Tract and that it probably does not avulse away from its valley as quickly as it does when it's in the Old Brahmaputra valley.

In the historical deltaic and climatic contexts described by Goodbred and Kuehl (2000), we know that sedimentation of the delta did not begin until at least 11ka when sea-level was rising rapidly. Goodbred and Kuehl also present evidence that suggests that the Brahmaputra River flowed in its western course, or the Brahmaputra-Jamuna valley, until ~7500 cal BP. From dates obtained in this study, we know that the Brahmaputra-Jamuna valley was occupied at ~6500, ~7800, and ~8800 cal BP, and that the Holocene Overbank Mud facies was being deposited at ~6800 cal BP in the Old Brahmaputra valley.

Ahmed et al. (2010) drilled near the village of Mymensingh, about 50 km southeast of BNGA081 along the path of the Old Brahmaputra River, near the northeastern edge of the Madhupur Terrace. A radiocarbon date returned from this groundwater study is 4315 BP at ~10 m depth. Ahmed et al. reached the Pleistocene Madhupur clay just below the peat layer this date was obtained from. Goodbred and Kuehl (2000) bored further downstream of the Old Brahmaputra channel, near the confluence of the Old Brahmaputra and the Meghna rivers, and obtained a radiocarbon date of 7493 cal BP at about 35 m depth. These dates are comparable to dates from this study of ~6800 cal BP at ~40 m depth in the Old Brahmaputra valley.

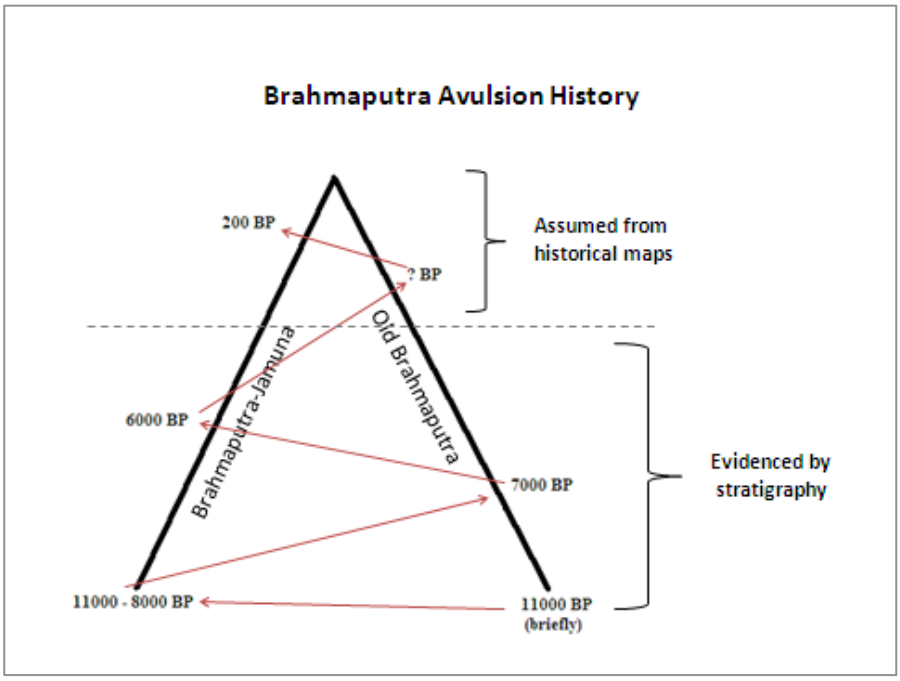

Figure 17: Conceptual illustration of occupations of Brahmaputra channel paths.

Assuming the river is always in the Brahmaputra-Jamuna valley or the Old Brahmaputra valley for simplicity, channel fill deposits in cores from this study confirm 3 major avulsions and at least 2 occupations per valley during the last 11,000 years of deltaic aggradation (Fig. 17). We know that at least 2 more avulsions occurred in the last 6000 years – one is the historically known recent avulsion out of the Old Brahmaputra and back into the Brahmaputra-Jamuna valley, and the other is the avulsion that would have placed the river in the Old Brahmaputra leading up to that recent avulsion. This makes 5 major avulsions and 3 occupations per valley in the last 11,000 years, giving an avulsion frequency of 2200 years based on stratigraphic observations. Because of the possibility that some of the stratigraphic record may not be preserved, we find it reasonable to estimate 4-6 avulsions in the last 11,000 years, which gives a mean avulsion frequency of about 1800-2700 years. While external forcings like changes in the climate or tectonic regime may influence the behavior of the Brahmaputra River, these timescales serve as reasonable first-order estimates of occupation timescales throughout the Holocene.

CHAPTER V

CONCLUSIONS

The Brahmaputra River has infilled two valleys downstream of a nodal avulsion site in the upper delta plain of north-central Bangladesh. The Brahmaputra-Jamuna and Old Brahmaputra valleys are flanked by macroform topographic bounding surfaces that have persisted since at least the latest Pleistocene. Pleistocene-aged terraces consisting of oxidized sands and stiff muds flank the Brahmaputra-Jamuna valley and the west side of the Old Brahmaputra valley, and the muddy Dauki Foredeep basin flanks the east side of the Old Brahmaputra valley. Each of these incised paleovalleys is filled with Holocene-aged fluvial sediments that display an overall fining-upward trend. The stratigraphy of these valleys is too complex to correlate at a fine scale, i.e. we cannot identify individual channel bars or correlate singular strata across the 3 km spacing of our boreholes. However, we have identified 8 distinct sedimentary facies that were deposited under different spatial and temporal conditions in this upper delta plain.

Transect A is composed primarily of sand-sized sediments that represent channel and bar, or fluvial braidbelt, deposits. Although floodplain muds are frequently preserved at the surface of boreholes, very few floodplain mud deposits are preserved in the deeper stratigraphy. This lack of mud in the subsurface suggests that throughout the Holocene, the river has been migrating laterally within its valley, constrained only by the macroform surfaces that bound it. Using the width-to-thickness aspect ratios of these valleys, the relative steepness of the valley walls, and the amount of subsurface mud preserved within each, we suggest that the Brahmaputra River is much more laterally mobile while it occupies the Brahmaputra-Jamuna valley than it is while it occupies either of the Old Brahmaputra sub-valleys.

Historical maps have documented the most recent avulsion of the Brahmaputra River at a node near the village of Dewanganj. Using subtleties within the distribution of sediments of Transect A, together with the surface morphology of the upper Bengal Delta plain, we have qualitatively reconstructed the Holocene avulsion processes and history of this river. In the Brahmaputra-Jamuna valley, the dominant river behavior responsible for building and reworking the stratigraphy is lateral migration and accretion, and the avulsion periodicity is high, i.e. the river avulses into this valley and does not avulse away quickly because it is able to continually

erode into the friable western valley margin. In the Old Brahmaputra valley, the dominant river behavior is relatively rapid channel aggradation with little lateral motion that results in a lower recurrence of avulsions, i.e. the river avulses away from this valley and does not return quickly. Essentially, the river has occupied both valleys the same number of times, but differences in the bounding topographic features, their respective lithological characters, and the dimensions of these valleys have caused the river to behave differently in either valley.

APPENDIX A:

DIGITAL ELEVATION MODELS OF UPPER BENGAL DELTA

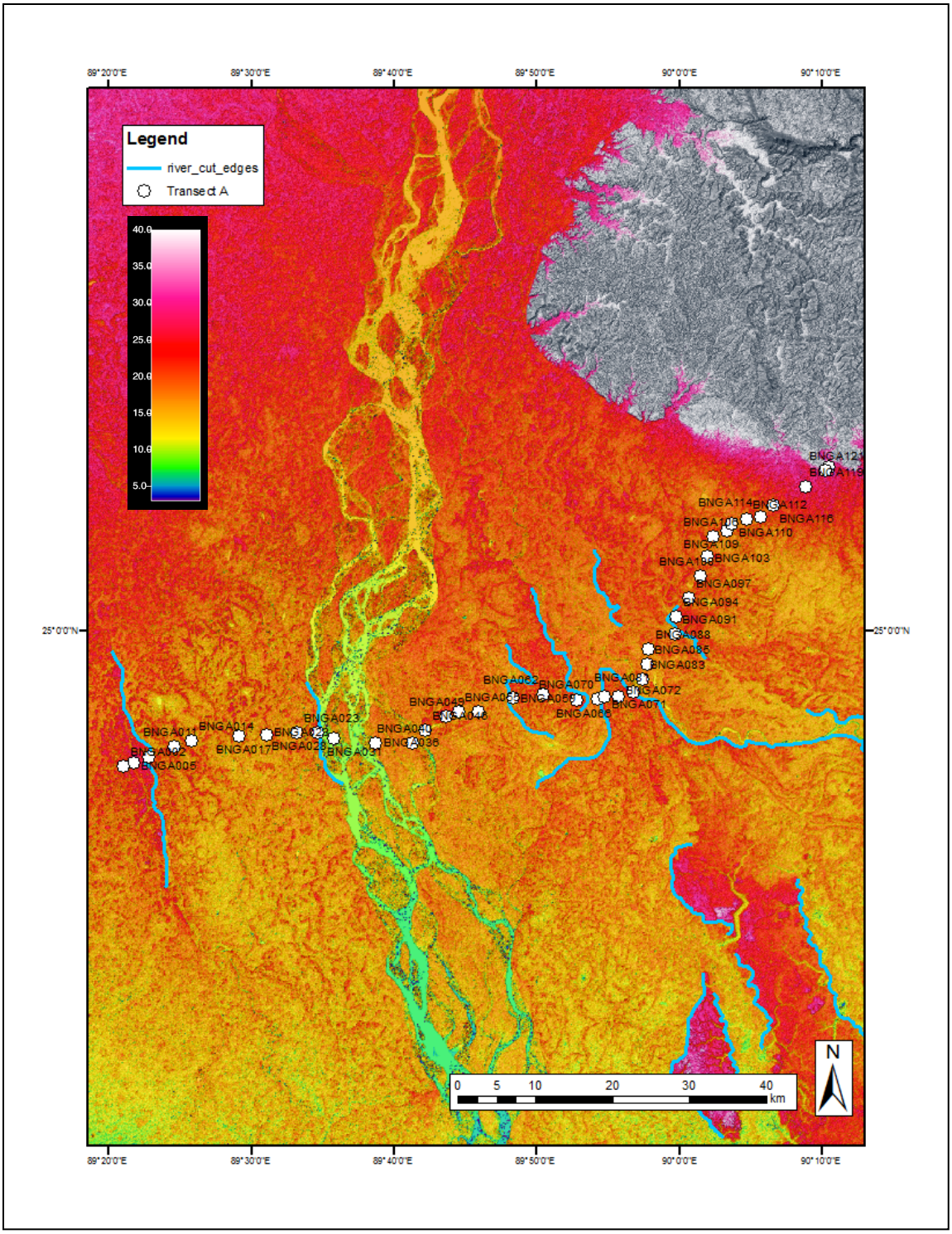

Appendix A.1 - DEM of Transect A. Figure provided by Haley Briel, BS 2012, Vanderbilt University.

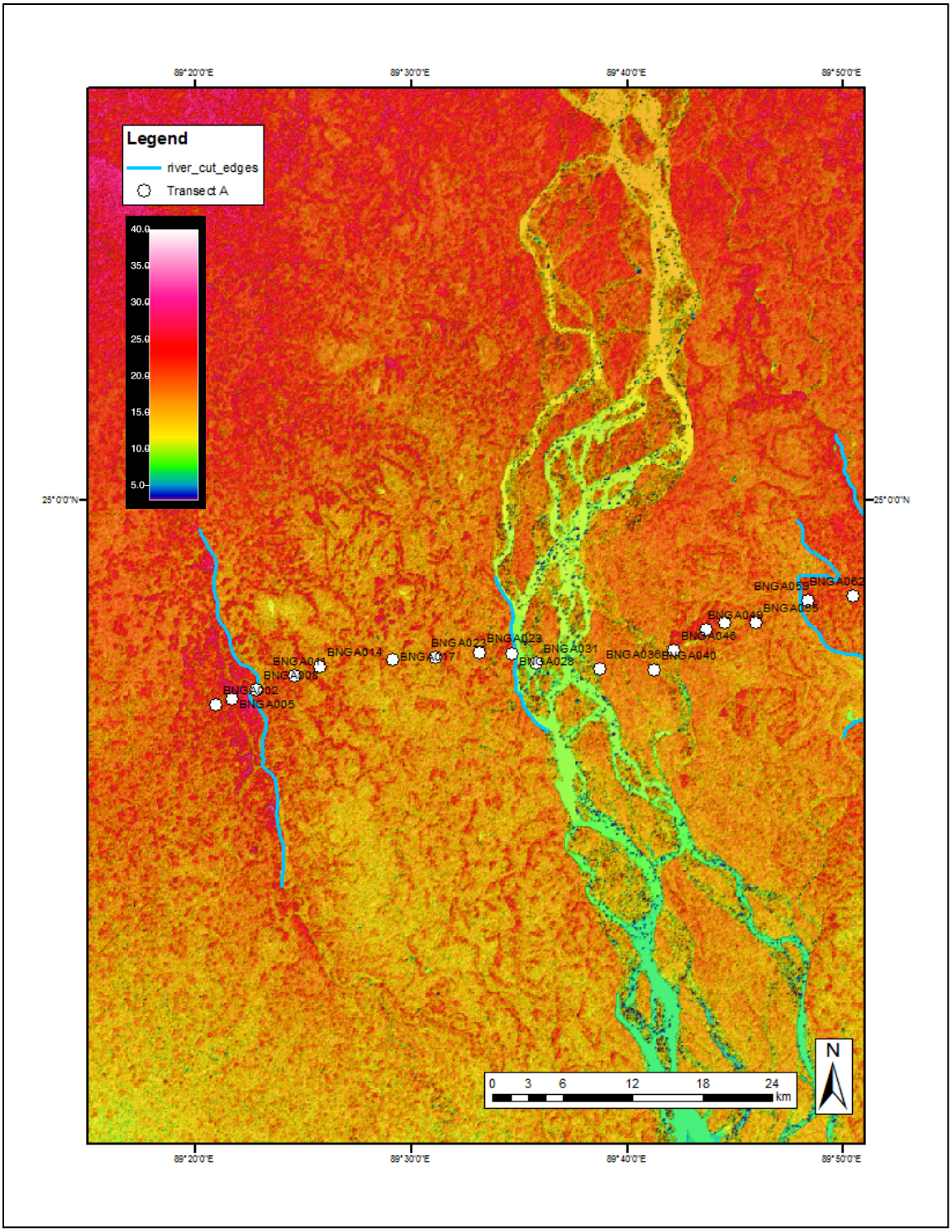

Appendix A.2 – DEM of Transect A boreholes 002-062. Figure provided by Haley Briel, BS 2012, Vanderbilt University.

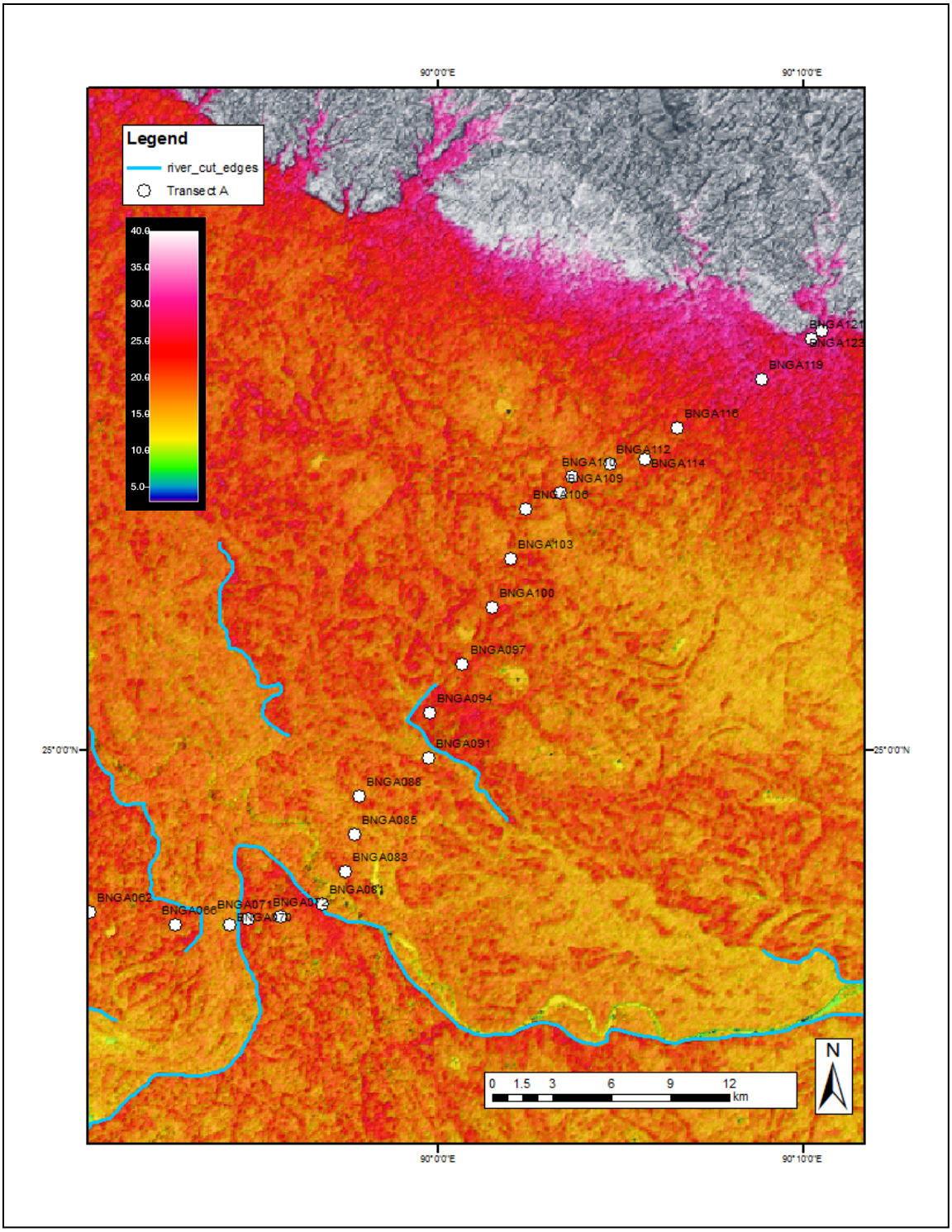

Appendix A.3 – DEM of Transect A boreholes 062-123. Figure provided by Haley Briel, BS 2012, Vanderbilt University.

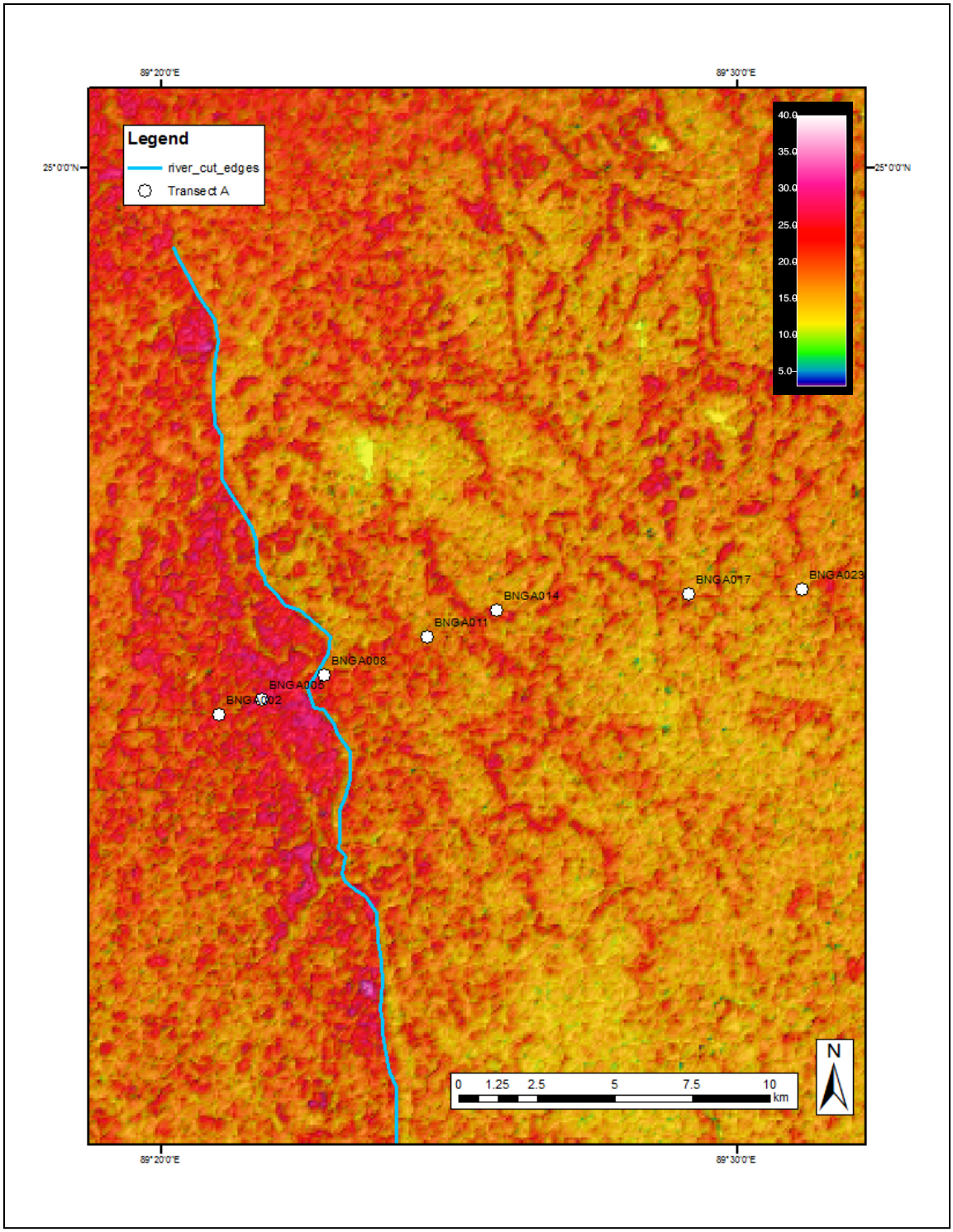

Appendix A.4 – DEM of Transect A boreholes 002-023. Figure provided by Haley Briel, BS 2012, Vanderbilt University.

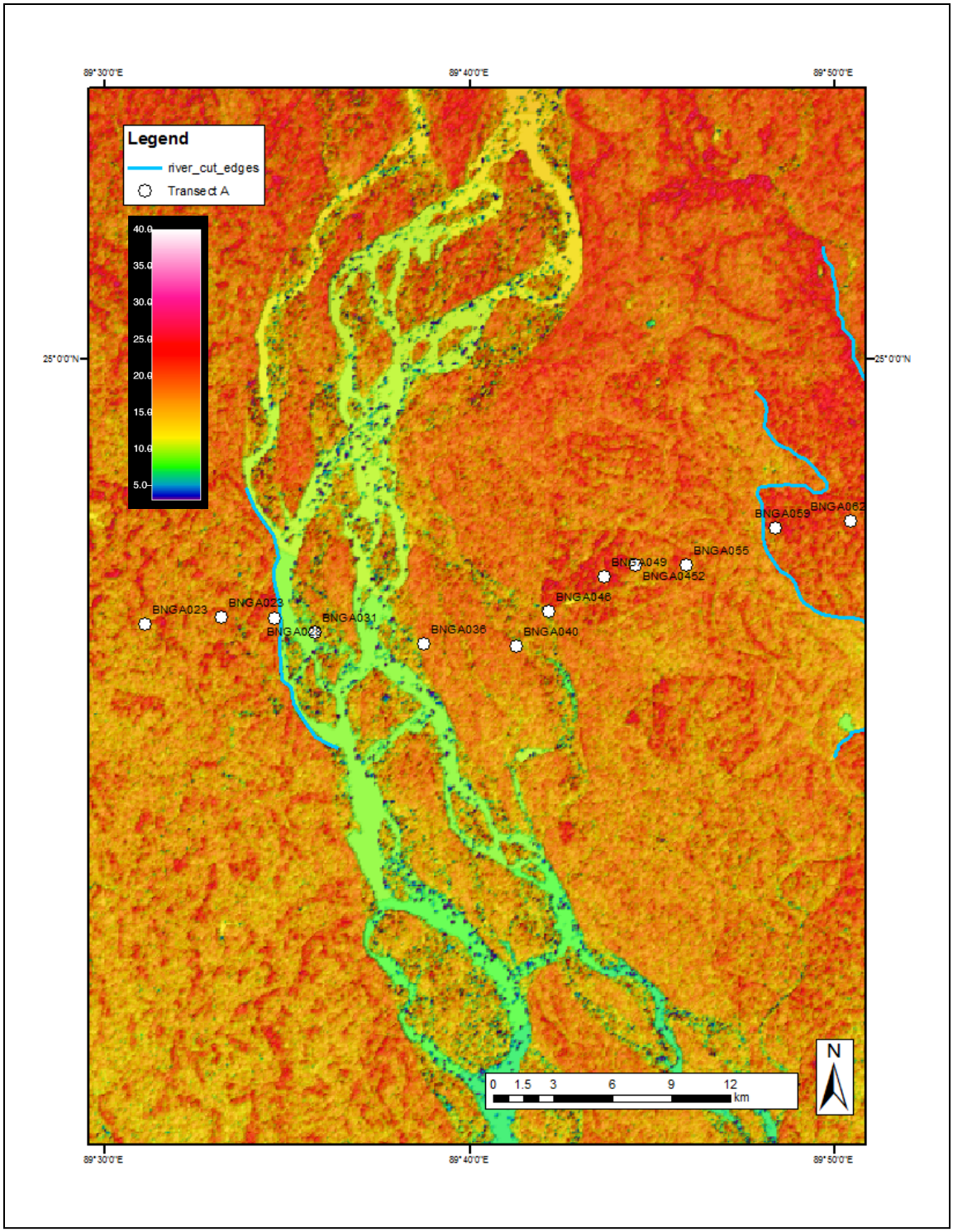

Appendix A.5 – DEM of Transect A boreholes 023-062. Figure provided by Haley Briel, BS 2012, Vanderbilt University.

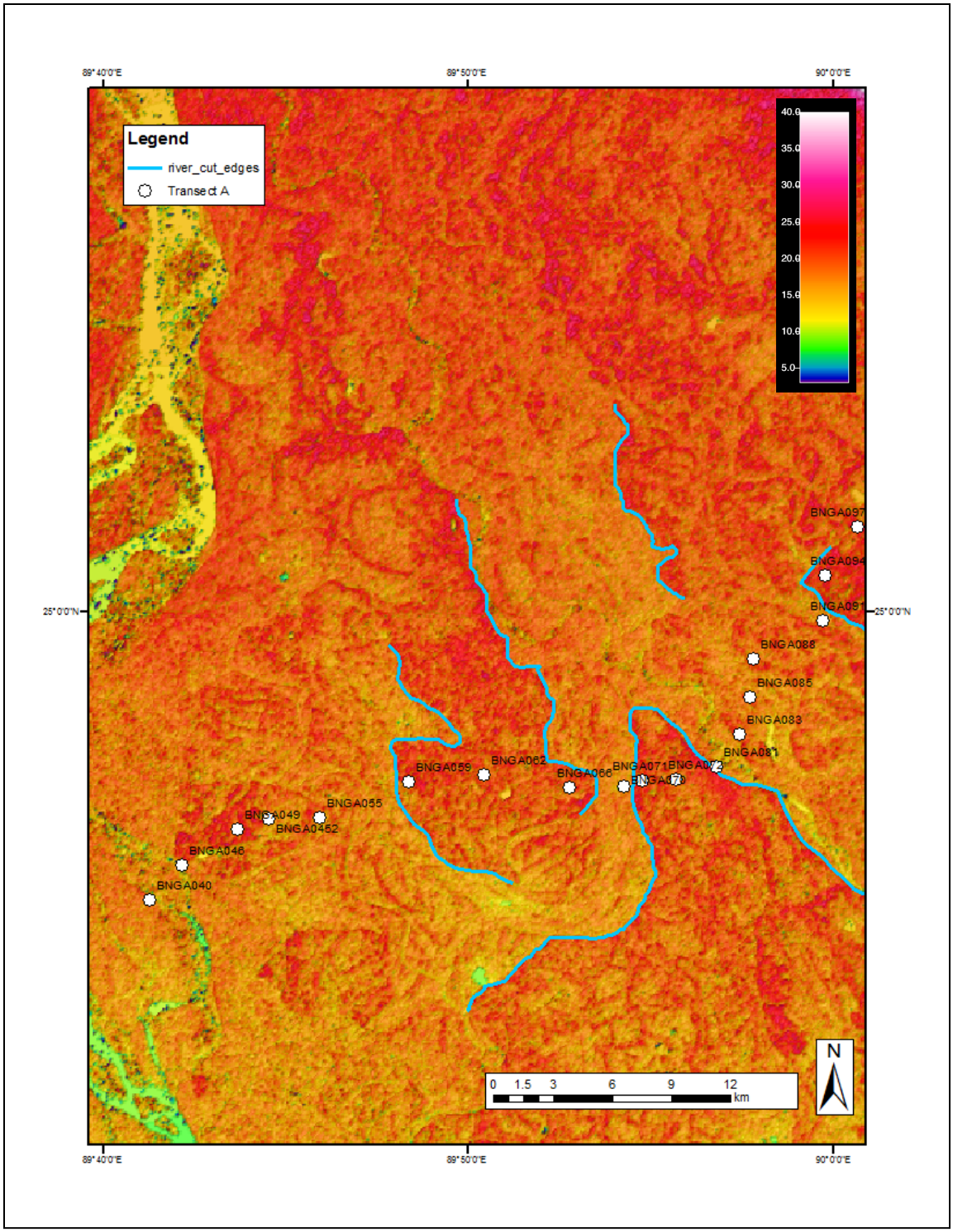

Appendix A.6 – DEM of Transect A boreholes 040-097. Figure provided by Haley Briel, BS 2012, Vanderbilt University.

REFERENCES

Ahmed, F.M., Bibi, H., Ishiga, H., Fukushima, T., and Maruoka, T., 2010. Geochemical study of Arsenic and other trace elements in groundwater and sediments of the Old Brahmaputra River plain, Bangladesh. Environmental Earth Sciences, 60(6), doi:10.1007/s12665-009-0270-7.

Alam, M., 1989. Geology and depositional history of Cenozoic sediments of the Bengal Basin of Bangladesh. Palaeogeography, palaeoclimatology, palaeoecology, 69, 125-139.

Alam, M.K., Shahidul Hasan, A.K.M., Khan, M.R., (Geological Survey of Bangladesh), and Whitney, J.W. (United States Geological Survey), 1990. Geological map of Bangladesh.

Baki, A.B.M., and Gan, T.Y., 2012. Riverbank migration and island dynamics of the braided Jamuna River of the Ganges–Brahmaputra basin using multi-temporal Landsat images. Quaternary International, doi:10.1016/j.quaint.2012.03.016.

Best, J.L., Ashworth, P.J., Sarker, M.H., and Roden, J.E., 2007, The Brahmaputra-Jamuna River, Bangladesh. In: *Large Rivers: Geomorphology and Management.* John Wiley & Sons, Ltd., 395-433.

Bookhagen, B. and Burbank, D.W., 2010. Towards a complete Himalayan hydrologic budget: The spatiotemporal distribution of snowmelt and rainfall and their impact on river discharge. Journal of Geophysical Research, doi:10.1029/2009JF001426.

Bristow, C.S., 1999. Gradual avulsion, river metamorphosis and reworking by underfit streams: a modern example from the Brahmaputra River in Bangladesh and a possible ancient example in the Spanish Pyrenees. In: *Fluvial Sedimentology VI*. International Association of Sedimentologists, Special Publication 28, p. 221-230.

Coleman, J.A., 1969. Brahmaputra River: channel processes and sedimentation. Sedimentary Geology. 3, 129-239.

Curray, J.R., 1991. Geological history of the Bengal geosyncline. Journal of the Association of Exploration Geophysics, 12, 209-219.

Delft Hydraulics and others, 1996. River Survey Project, Flood Action Plan 24, Special Report No. 18: Sediment Rating Curves and Balances. Dhaka, Water Resources Planning Organization.

Environmental and GIS Support Project for Water Sector Planning (EGIS), 1997. Morphological Dynamics of the Brahmaputra-Jamuna River. Prepared for Water Resources Planning Organization, Dhaka, Bangladesh, 76 pp.

Environment and GIS Support Project for Water Sector Planning (EGIS), 2000, Riverine chars in Bangladesh: Environmental dynamics and management issues. The University Press Limited, Dhaka, 86 p.

Garzanti, E., Vezzoli, G., Ando, S., France-Lanord, C., Singh, S., & Foster, G. (2004). Sand petrology and focused erosion in collision orogens: the Brahmaputra case. Earth and Planetary Science Letters, 220, 157-174. doi:10.1016/S0012-821X(04)00035-4.

Gibling, M.R., 2006. Width and thickness of fluvial channel bodies and valley fills in the geological record: A literature compilation and classification. Journal of Sedimentary Research, 76, 731-770.

Goodbred, S.L., and Kuehl, S.A., 2000. The significance of large sediment supply, active tectonism, and eustasy on margin sequence development: Late Quaternary stratigraphy and evolution of the Ganges-Brahmaputra delta. Sedimentary Geology, 133, 227-248.

Goodbred, S.L., Kuehl, S.A., Steckler, M., and Sarker, M.H., 2003. Controls on facies distribution and stratigraphic preservation in the Ganges-Brahmaputra delta sequence. Sedimentary Geology, 155, 301-316.

Hartzog, T.R., in prep. Controls, distribution, and significance of gravel in the Holocene stratigraphy of the Brahmaputra River.

Japan International Cooperation Agency (JICA), 1976. People's Republic of Bangladesh Jamuna Bridge Construction Report: Feasibility Study Report, 6, 16-20.

Johnson, S.Y. and Alam, A.M.N., 1991. Sedimentation and tectonics of the Sylhet trough, Bangladesh. Geological Society of America Bulletin. 103, 1513-1527.

Kim, W., Sheets, B.A., and Paola, C., 2010. Steering of experimental channels by lateral basin tilting. Basin Research, 22, 286-301.

Mètevier, F., Gaudemer, Y., Tapponnier, P., and Klein, M., 1999. Mass accumulation rates in Asia, during the Cenozoic. Geophysical Journal International, 137, 280-318.

Morgan, J.P. and McIntire, W.G., 1959. Quaternary geology of the Bengal Basin, East Pakistan and India. Geological Society of America Bulletin. 70, 319-342.

Nicholls, R.J. and Goodbred, S.L., 2004. Towards integrated assessment of the Ganges-Brahmaputra Delta. Conference Proceedings: International Conference on Asian Marine Geology.

Oldham, R.D., 1899. Report of the great earthquake of 12th June, 1897. Memoirs of the Geological Survey of India, 29, 377 p.

Rashid, T., Monsur, M.H., and Suzuki, S., 2006. A review on the Quaternary characteristics of Pleistocene Tracts of Bangladesh. Earth Science Reports, 13, 1-13.

Rennel, J., 1776. An actual survey, of the provinces of Bengal, Bahar and c. East India Company, map.

Sarker, M.H., Huque, I., Alam, M., and Koudstaal, R., 2003, Rivers, chars and char dwellers of Bangladesh. International Journal of River Basin Management 1:1, 61-80.

Sarker, M.H. and Thorne, C.R, 2006. Morphological response of the Brahmaputra-Padma-Lower Meghna river system to the Assam earthquake of 1950. In: Braided Rivers: Process, Deposits, Ecology and Management. DOI: 10.1002/9781444304374.ch14

Singh, S.K. and France-Lanord, C., 2002. Tracing the distribution of erosion in the Brahmaputra watershed from isotopic compositions of stream sediments. Earth and Planetary Science Letters, 202, 645-662.

Slingerland, R. and Smith, N.D., 2004. River avulsions and their deposits. Annual Review of Earth and Planetary Sciences, 32, 257-285.

Steckler, M.S., Akhter, S.H., Seeber, L., Bilham, R., Kogan, M., Masson, F., Maurin, T., Mondal, D., Agostinetti, N.P., Rangin, C., and Saha, P., 2012. GPS Velocities and Structure Across the Burma Accretionary Prism and Shillong Anticline in Bangladesh. Abstract T51F-2667presented at 2012 Fall Meeting, AGU, San Francisco, Calif., 3-7 Dec.

Stuiver, M. and Reimer, P.J., 1993. Extended ^{14}C data base and revised CALIB 3.0 ^{14}C age calibration program, Radiocarbon, 35, 215-230.

Sukhija, M.N., Rao, D.V., Nagabhushanam, P., Hussain, S., Chadha, R.K., and Gupta, H.K, 1999. Timing and return period of major paleoseismic events in the Shillong Plateau, India. Tectonophysics, 308, 53-65.

Thorne, CR., Russell, A.P.G., and Alam, M.K., 1993. Planform pattern and channel evolution of the Brahmaputra River, Bangladesh. Geological Society, London, Special Publications 1993, v. 75, p. 257-276.

Umitsu, M., 1993. Late Quaternary sedimentary environments and landforms in the Ganges delta. Sedimentary Geology, 83, 177–186.